

Spectral Measures for G_2

DAVID E. EVANS AND MATHEW PUGH

School of Mathematics, Cardiff University,
Senghennydd Road, Cardiff CF24 4AG, Wales, U.K.

September 26, 2021

Abstract

Spectral measures provide invariants for braided subfactors via fusion modules. In this paper we study joint spectral measures associated to the rank two Lie group G_2 , including the McKay graphs for the irreducible representations of G_2 and its maximal torus, and fusion modules associated to all known G_2 modular invariants.

Contents

1	Introduction	1
2	Representation theory of G_2 and its maximal torus	4
2.1	Spectral measures over different domains	7
3	Spectral measures for $\mathcal{WA}_\infty(G_2)$	9
3.1	Joint spectral measure for $\mathcal{WA}_\infty(G_2)$ over \mathbb{T}^2	10
3.2	Joint spectral measure for $\mathcal{WA}_\infty(G_2)$ on \mathfrak{D}	10
3.3	Spectral measure for $\mathcal{WA}_\infty(G_2)$ on \mathbb{R}	13
4	Spectral measures for $\mathcal{A}_\infty(G_2)$	14
4.1	Joint spectral measure for $\mathcal{A}_\infty(G_2)$ over \mathbb{T}^2	15
4.2	Spectral measure for $\mathcal{A}_\infty(G_2)$ on \mathbb{R}	16
5	Joint spectral measures for nimrep graphs associated to G_2 modular invariants	17
5.1	Graphs $\mathcal{A}_k(G_2)$, $k \leq \infty$	19
5.2	Exceptional Graph $\mathcal{E}_3(G_2)$: $(G_2)_3 \rightarrow (E_6)_1$	21
5.3	Exceptional Graph $\mathcal{E}_3^M(G_2)$: $(G_2)_3 \rightarrow (E_6)_1 \rtimes \mathbb{Z}_3$	24
5.4	Exceptional Graph $\mathcal{E}_4(G_2)$: $(G_2)_4 \rightarrow (D_7)_1$	26
5.5	Exceptional Graph $\mathcal{E}_4^M(G_2)$: $(G_2)_4 \rightarrow (D_7)_1 \rtimes \mathbb{Z}_2$	30
5.6	Exceptional Graph $\mathcal{E}_4^*(G_2)$	31
	References	32

1 Introduction

Spectral measures associated to the compact Lie group $A_1 = SU(2)$ and its maximal torus, nimrep graphs associated to the $SU(2)$ modular invariants, and the McKay graphs

for finite subgroups of $SU(2)$ were studied in [1] using information about the generating series of the moments of the spectral measure and the Jones series which is related to the Poincaré series of the subfactor planar algebra associated to the graph (see e.g. [30]). In [21, 22] the authors studied spectral measures associated to the compact Lie groups $A_1 = SU(2)$ and $A_2 = SU(3)$ and their maximal tori, nimrep graphs associated to the $SU(2)$ and $SU(3)$ modular invariants, and the McKay graphs for finite subgroups of $SU(2)$ and $SU(3)$, using braided subfactor theory. Spectral measures associated to the compact rank two Lie groups B_2 and C_2 are studied in [25], and for other compact rank two Lie groups in [24]. In this paper and its sequel [23] we focus on the Lie group $G_2 = \text{Aut}(\mathbb{O})$, the automorphism group of the octonions \mathbb{O} . It is a simply connected, compact, real rank two Lie group of dimension 14 and is the smallest of the exceptional Lie groups. It is isomorphic to the subgroup of $SO(7)$ that fixes any particular vector in its 8-dimensional real spinor representation. We determine spectral measures and joint spectral measures for (the adjacency matrices of) various graphs related to the Lie group G_2 : the McKay (or representation) graphs for the irreducible representations of G_2 and its maximal torus \mathbb{T}^2 , nimrep graphs or fusion modules associated to the G_2 modular invariants, and in the sequel [23], the McKay graphs for finite subgroups of G_2 .

Suppose A is a unital C^* -algebra with state φ . If $a \in A$ is a self-adjoint operator then there exists a compactly supported probability measure ν_a , the spectral measure of a , on the spectrum $\sigma(a) \subset \mathbb{R}$ of a , uniquely determined by its moments $\varphi(a^m) = \int_{\sigma(a)} x^m d\nu_a(x)$, for all non-negative integers m . Note that ν_a depends on the choice of state φ on A . In the cases we consider, the C^* -algebra A will be a space of operators which act on the following Hilbert space H . For the McKay graphs for irreducible representations of G_2 we have $H = \ell^2(\mathbb{N}) \otimes \ell^2(\mathbb{N})$, whilst for the irreducible representations of its maximal torus \mathbb{T}^2 we have $H = \ell^2(\mathbb{Z}) \otimes \ell^2(\mathbb{Z})$. For a nimrep graph \mathcal{G} (either associated to a G_2 modular invariant or the McKay graph for finite subgroups of G_2) with vertex set \mathcal{G}_0 , we take $H = \ell^2(\mathcal{G}_0)$.

As G_2 has rank two, its characters are functions on the maximal torus \mathbb{T}^2 of G_2 . For $SU(2)$ and $SU(3)$ it was convenient to determine the spectral measures for the operator a given by the adjacency matrices of the various graphs related to these groups (the McKay graphs for the irreducible representations of the group and its maximal torus, nimrep graphs associated to modular invariants, and the McKay graphs for finite subgroups) by first determining corresponding measures ε_a over the maximal tori of $SU(2)$ or $SU(3)$ respectively. This approach is described as a spectral measure blowup in [2]. In the case of G_2 , the maximal torus \mathbb{T}^2 has dimension one greater than the spectrum $\sigma(a) \subset \mathbb{R}$, so that there is a loss of dimension when passing from the measure ε_a to ν_a . This means that there is an infinite family of measures ε_a over \mathbb{T}^2 which correspond to the spectral measure ν_a (details of the relation between ε_a and ν_a are given in Section 2.1).

In order to remove this ambiguity, we also consider measures over the joint spectrum $\sigma(a, b) \subset \sigma(a) \times \sigma(b) \subset \mathbb{R}^2$ of commuting self-adjoint operators a and b . The abelian C^* -algebra B generated by a , b and the identity 1 is isomorphic to $C(X)$, where X is the spectrum of B . Then the joint spectrum is defined as $\sigma(a, b) = \{(a(x), b(x)) | x \in X\}$. In fact, one can identify the spectrum X with its image $\sigma(a, b)$ in \mathbb{R}^2 , since the map $x \mapsto (a(x), b(x))$ is continuous and injective, and hence a homeomorphism since X is compact [39]. In the case where the operators a , b act on a finite-dimensional Hilbert space, this is the set of all pairs of real numbers (λ_a, λ_b) for which there exists a non-

zero vector ϕ such that $a\phi = \lambda_a\phi$, $b\phi = \lambda_b\phi$. Then there exists a compactly supported probability measure $\tilde{\nu}_{a,b}$ on $\sigma(a, b)$, which is uniquely determined by its cross moments

$$\varphi(a^m b^n) = \int_{\sigma(a,b)} x^m y^n d\tilde{\nu}_{a,b}(x, y), \quad (1)$$

for all non-negative integers m, n . The spectral measure for a is then given by the pushforward $(p_a)_*(\tilde{\nu}_{a,b})$ of the joint spectral measure $\tilde{\nu}_{a,b}$ under the orthogonal projection p_a onto the spectrum $\sigma(a)$.

To study the spectral measures for the nimrep graphs associated to the G_2 modular invariants, we use the theory of braided subfactors and α -induction, which we now briefly review. For a fuller discussion on braided subfactors and α -induction see [6, 7]. The Verlinde algebra of G_2 at level k is represented by a non-degenerately braided system of endomorphisms ${}_N\mathcal{X}_N$ on a type III₁ factor N . Its fusion rules $\{N_{\lambda}^{\mu}\}$ reproduce exactly those of the positive energy representations of the loop group of G_2 at level k , $N_{\lambda}N_{\mu} = \sum_{\nu} N_{\lambda\nu}^{\mu} N_{\nu}$. Furthermore its statistics generators S, T obtained from the braided tensor category ${}_N\mathcal{X}_N$ match exactly those of the Kač-Peterson modular S, T matrices which perform the conformal character transformations (see footnote 2 in [6]). From the Verlinde formula we see that this family $\{N_{\lambda}\}$ of commuting normal matrices can be simultaneously diagonalised, i.e. $N_{\lambda} = \sum_{\sigma} (S_{\sigma,\lambda}/S_{\sigma,0}) S_{\sigma} S_{\sigma}^*$, where the summation is over each $\sigma \in {}_N\mathcal{X}_N$ and 0 is the trivial representation. The intriguing aspect being that the eigenvalues $S_{\sigma,\lambda}/S_{\sigma,0}$ and eigenvectors $S_{\sigma} = \{S_{\sigma,\mu}\}_{\mu}$ are described by the modular S matrix.

A braided subfactor is an inclusion $N \subset M$ where the dual canonical endomorphism decomposes as a finite combination of elements of the Verlinde algebra, i.e. a finite combination of endomorphisms in ${}_N\mathcal{X}_N$. Such subfactors yield modular invariants through the procedure of α -induction which allows two extensions of λ on N , depending on the use of the braiding or its opposite, to endomorphisms $\alpha_{\lambda}^{\pm} \in {}_M\mathcal{X}_M^{\pm}$ of M , so that the matrix $Z_{\lambda,\mu} = \langle \alpha_{\lambda}^+, \alpha_{\mu}^- \rangle$ is a modular invariant [8, 5, 16]. The systems ${}_M\mathcal{X}_M^{\pm}$ are called the chiral systems, whilst the intersection ${}_M\mathcal{X}_M^0 = {}_M\mathcal{X}_M^+ \cap {}_M\mathcal{X}_M^-$ is called the neutral system. Then ${}_M\mathcal{X}_M^0 \subset {}_M\mathcal{X}_M^{\pm} \subset {}_M\mathcal{X}_M$, where ${}_M\mathcal{X}_M \subset \text{End}(M)$ denotes a system of endomorphisms consisting of a choice of representative endomorphisms of each irreducible subsector of sectors of the form $[\iota\lambda\bar{\iota}]$, $\lambda \in {}_N\mathcal{X}_N$, where $\iota : N \hookrightarrow M$ is the inclusion map. Although ${}_N\mathcal{X}_N$ is assumed to be braided, the systems ${}_M\mathcal{X}_M^{\pm}$ or ${}_M\mathcal{X}_M$ are not braided in general. The action of each N - N sector $\lambda \in {}_N\mathcal{X}_N$ on the M - N sectors ${}_M\mathcal{X}_N$ produces a nimrep (non-negative integer matrix representation of the original Verlinde algebra) G_{λ} , i.e. $G_{\lambda}G_{\mu} = \sum_{\nu} N_{\lambda\nu}^{\mu} G_{\nu}$. The spectrum of (each) G_{λ} reproduces exactly the diagonal part of the modular invariant [9]. Since the nimreps are a family of commuting matrices, they can be simultaneously diagonalised and thus the eigenvectors ψ_{σ} are the same for the nimrep graphs G_{λ} for all $\lambda \in {}_N\mathcal{X}_N$. We have $G_{\lambda} = \sum_{\sigma} (S_{\sigma,\lambda}/S_{\sigma,0}) \psi_{\sigma} \psi_{\sigma}^*$, where the summation is over each $\sigma \in {}_N\mathcal{X}_N$ with multiplicity given by the modular invariant, i.e. the spectrum of G_{λ} is given by $\{S_{\sigma,\lambda}/S_{\sigma,0}$ with multiplicity $Z_{\sigma,\sigma}\}$. The set of μ with multiplicity $Z_{\mu,\mu}$ is called the set of exponents of G .

Along with the identity invariants for G_2 for all levels k , there are two exceptional invariants due to conformal embeddings at levels 3, 4 [12] and another exceptional invariant at level 4 [41]. These are all the known G_2 modular invariants. Since the centre of G_2 is trivial, there are no orbifold modular invariants. This list was shown to be complete for all prime heights $k+4$ such that $k+4 \equiv 5, 7 \pmod{12}$ [38], and for all other $k \leq 31$ [27].

The paper is organised as follows. In Section 2 we describe the representation theory of G_2 and its maximal torus \mathbb{T}^2 , and in particular focus on the fundamental representations of G_2 . In Section 2.1 we discuss spectral measures for G_2 over different domains, showing how measures over a region in the complex plane yields a unique W -invariant measure over \mathbb{T}^2 , where W is the Weyl group of G_2 .

In Section 3 we determine the (joint) spectral measures associated to the (adjacency matrices of the) McKay graphs given by the action of the irreducible characters of G_2 on its maximal torus \mathbb{T}^2 , and in Section 4 the (joint) spectral measures associated to the (adjacency matrices of the) McKay graphs of G_2 itself. In both cases we focus on the fundamental representations of G_2 , and determine these (joint) spectral measures over \mathbb{T}^2 and the (joint) spectrum of these adjacency matrices. Finally in Section 5 we determine joint spectral measures over \mathbb{T}^2 for nimrep graphs arising from G_2 braided subfactors.

2 Representation theory of G_2 and its maximal torus

The irreducible representations $\lambda_{(\mu_1, \mu_2)}$ of G_2 are indexed by pairs $(\mu_1, \mu_2) \in \mathbb{N}^2$ such that $\mu_1 \geq \mu_2$. We denote by $\rho_1 = \lambda_{(1,0)}$ the fundamental representation of G_2 of dimension 7, where $\rho_1(G_2) \subset SO(7)$. The maximal torus of $SO(7)$ is $T = \text{diag}(D(\omega_1), D(\omega_2), D(\omega_3), 1)$, for $\omega_i \in \mathbb{T}$, where $D(\omega_i) = \begin{pmatrix} \text{Re}(\omega_i) & -\text{Im}(\omega_i) \\ \text{Im}(\omega_i) & \text{Re}(\omega_i) \end{pmatrix}$, and the maximal torus of G_2 is the subset of T such that $\omega_1 + \omega_2 + \omega_3 = 0$, which is isomorphic to \mathbb{T}^2 . Then the restriction of ρ_1 to \mathbb{T}^2 is given by the 7×7 block-diagonal matrix

$$(\rho_1|_{\mathbb{T}^2})(\omega_1, \omega_2) = \text{diag}(D(\omega_1), D(\omega_2^{-1}), D(\omega_1^{-1}\omega_2), 1), \quad (2)$$

for $(\omega_1, \omega_2) \in \mathbb{T}^2$. We also denote by $\rho_2 = \lambda_{(1,1)}$ the second fundamental representation of G_2 , the adjoint representation which has dimension 14.

The Lie group $SU(3)$ is a subgroup of G_2 . The generating function for the $SU(3) \subset G_2$ branching rules was determined in [28]. In particular, the fundamental representations ρ_1, ρ_2 of G_2 branch into the following irreducible $SU(3)$ representations:

$$\rho_1 \longrightarrow \Sigma_1 \oplus \Sigma_3 \oplus \Sigma_3^*, \quad \rho_2 \longrightarrow \Sigma_3 \oplus \Sigma_3^* \oplus \Sigma_8. \quad (3)$$

The representations Σ_3, Σ_3^* are conjugate to one another and are the fundamental three-dimensional representations of $SU(3)$. The eight-dimensional representation Σ_8 is the adjoint representation of $SU(3)$ and is obtained from the product of the fundamental representations by removing one copy of the trivial representation Σ_1 , since $\Sigma_3 \otimes \Sigma_3^* = \Sigma_1 \oplus \Sigma_8$. Then from (3) the restriction of ρ_2 to \mathbb{T}^2 is given by the 14×14 block-diagonal matrix

$$(\rho_2|_{\mathbb{T}^2})(\omega_1, \omega_2) = \text{diag}(D(\omega_1), D(\omega_2^{-1}), D(\omega_1^{-1}\omega_2), D(1), D(\omega_1\omega_2), D(\omega_1^2\omega_2^{-1}), D(\omega_1^{-1}\omega_2^2)), \quad (4)$$

for $(\omega_1, \omega_2) \in \mathbb{T}^2$.

Let $\{\chi_{(\mu_1, \mu_2)}\}_{\mu_1, \mu_2 \in \mathbb{N}; \mu_1 \geq \mu_2}, \{\sigma_{(\mu_1, \mu_2)}\}_{\mu_1, \mu_2 \in \mathbb{Z}}$ be the irreducible characters of G_2, \mathbb{T}^2 respectively, where $\chi_{(\mu_1, \mu_2)} := \chi_{\lambda_{(\mu_1, \mu_2)}}$. The characters $\chi_{(\mu_1, \mu_2)}$ of G_2 are self-conjugate and thus are maps from the torus \mathbb{T}^2 to an interval $I_\mu := \chi_\mu(\mathbb{T}^2) \subset \mathbb{R}$. For $\omega_i \in \mathbb{T}, \mu_i \in \mathbb{Z}$, the characters of \mathbb{T}^2 are given by $\sigma_{(\mu_1, \mu_2)}(\omega_1, \omega_2) = \omega_1^{\mu_1} \omega_2^{\mu_2}$, and satisfy $\overline{\sigma_{(\mu_1, \mu_2)}} = \sigma_{(-\mu_1, -\mu_2)}$. If

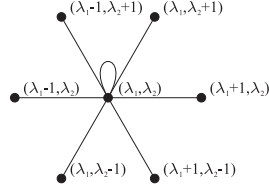


Figure 1: Multiplication by $\rho_1|_{\mathbb{T}^2}$

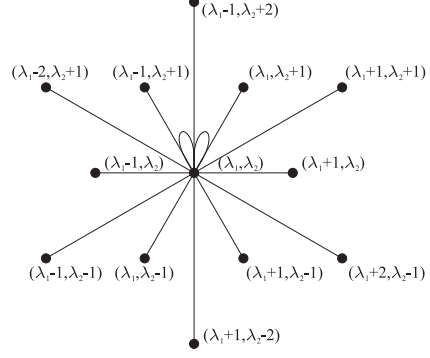


Figure 2: Multiplication by $\rho_2|_{\mathbb{T}^2}$

σ_1, σ_2 is the restriction of $\chi_1 := \chi_{(1,0)}$, $\chi_2 := \chi_{(1,1)}$ respectively to \mathbb{T}^2 , we have from (2) and (4) that

$$\sigma_1 = \chi_1|_{\mathbb{T}^2} = \sigma_{(0,0)} + \sigma_{(1,0)} + \sigma_{(-1,0)} + \sigma_{(0,-1)} + \sigma_{(0,1)} + \sigma_{(-1,1)} + \sigma_{(1,-1)}, \quad (5)$$

$$\sigma_2 = \chi_2|_{\mathbb{T}^2} = \sigma_1 + \sigma_{(0,0)} + \sigma_{(1,1)} + \sigma_{(-1,-1)} + \sigma_{(2,-1)} + \sigma_{(-2,1)} + \sigma_{(1,-2)} + \sigma_{(-1,2)}. \quad (6)$$

Then

$$\sigma_1 \sigma_{(\mu_1, \mu_2)} = \sigma_{(\mu_1, \mu_2)} + \sigma_{(\mu_1+1, \mu_2)} + \sigma_{(\mu_1-1, \mu_2)} + \sigma_{(\mu_1, \mu_2-1)} + \sigma_{(\mu_1, \mu_2+1)} + \sigma_{(\mu_1-1, \mu_2+1)} + \sigma_{(\mu_1+1, \mu_2-1)}, \quad (7)$$

for any $\mu_1, \mu_2 \in \mathbb{Z}$.

The McKay graph for an irreducible representation λ of a group G is the graph whose vertices are labelled by the irreducible representations of G , and which, for any two irreducible representations λ_1, λ_2 of G , has $N_{\lambda_1, \lambda_2}^{\lambda_1}$ (directed) edges from λ_1 to λ_2 , where the decomposition of $\lambda \lambda_1$ into irreducible contains $N_{\lambda, \lambda_2}^{\lambda_1}$ copies of λ_2 . The McKay graph of \mathbb{T}^2 for the first fundamental representation ρ_1 is identified with the infinite graph $W\mathcal{A}_{\infty}^{\rho_1}(G_2)$, illustrated in Figure 3, whose vertices may be labeled by pairs $(\mu_1, \mu_2) \in \mathbb{Z}^2$ such that there is an edge from (μ_1, μ_2) to (μ_1, μ_2) , $(\mu_1 + 1, \mu_2)$, $(\mu_1 - 1, \mu_2)$, $(\mu_1, \mu_2 - 1)$, $(\mu_1, \mu_2 + 1)$, $(\mu_1 - 1, \mu_2 + 1)$ and $(\mu_1 + 1, \mu_2 - 1)$.

Similarly, the McKay graph of \mathbb{T}^2 for the second fundamental representation ρ_2 is identified with the infinite graph $W\mathcal{A}_{\infty}^{\rho_2}(G_2)$, illustrated in Figure 4, where multiplication by ρ_2 corresponds to the edges illustrated in Figure 2. These graphs $W\mathcal{A}_{\infty}^{\rho}(G_2)$ are essentially W -unfolded versions of the graphs $\mathcal{A}_{\infty}^{\rho}(G_2)$, where W denotes the Weyl group D_{12} of G_2 .

By [18, §3.5], $(\bigotimes_{\mathbb{N}} M_7)^{\mathbb{T}^2} \cong A(W\mathcal{A}_{\infty}^{\rho_1}(G_2))$ and $(\bigotimes_{\mathbb{N}} M_{14})^{\mathbb{T}^2} \cong A(W\mathcal{A}_{\infty}^{\rho_2}(G_2))$. Here $A(\mathcal{G}) = \bigcup_k A(\mathcal{G})_k$ is the path algebra of the graph \mathcal{G} , where $A(\mathcal{G})_k$ is the algebra generated by pairs (η_1, η_2) of paths from the distinguished vertex $*$ such that $r(\eta_1) = r(\eta_2)$ and $|\eta_1| = |\eta_2| = k$, with multiplication defined by $(\eta_1, \eta_2) \cdot (\eta'_1, \eta'_2) = \delta_{\eta_2, \eta'_1}(\eta_1, \eta'_2)$. We now consider instead the fixed point algebra of $\bigotimes_{\mathbb{N}} M_7, \bigotimes_{\mathbb{N}} M_{14}$ under the action of the group G_2 given by the fundamental representations ρ_1, ρ_2 respectively, where G_2 acts by conjugation on each factor in the infinite tensor product.

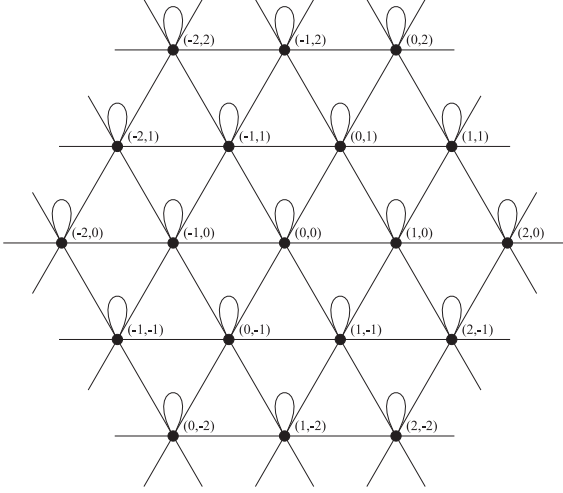


Figure 3: Infinite graph $W A_{\infty}^{\rho_1}(G_2)$

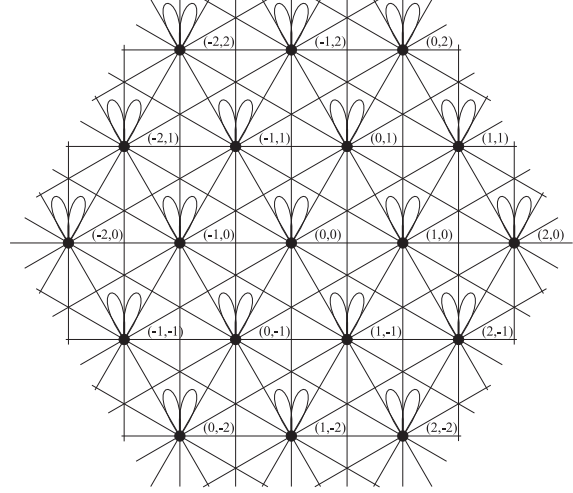


Figure 4: Infinite graph $W A_{\infty}^{\rho_2}(G_2)$

The characters $\{\chi_{(\mu_1, \mu_2)}\}_{\mu_1, \mu_2 \in \mathbb{N}; \mu_1 \geq \mu_2}$ of G_2 satisfy

$$\chi_1 \chi_{(\mu_1, \mu_2)} = \begin{cases} \chi_{(\mu_1, \mu_2)} + \chi_{(\mu_1+1, \mu_2)} + \chi_{(\mu_1-1, \mu_2)} + \chi_{(\mu_1, \mu_2-1)} + \chi_{(\mu_1, \mu_2+1)} \\ \quad + \chi_{(\mu_1-1, \mu_2+1)} + \chi_{(\mu_1+1, \mu_2-1)} & \text{if } \mu_1 \neq \mu_2, \\ \chi_{(\mu_1+1, \mu_2)} + \chi_{(\mu_1, \mu_2-1)} + \chi_{(\mu_1+1, \mu_2-1)} & \text{if } \mu_1 = \mu_2, \end{cases}$$

$$\chi_2 \chi_{(\mu_1, 0)} = \begin{cases} \chi_1 \chi_{(\mu_1, \mu_2)} + \chi_{(\mu_1+1, 1)} + \chi_{(\mu_1-2, 1)} + \chi_{(\mu_1-1, 2)} & \text{if } \mu_1 \neq \mu_2, \mu_2 + 1, \\ \chi_{(1, 1)} & \text{if } \mu_1 = 0, \\ \chi_{(1, 0)} + \chi_{(2, 0)} + \chi_{(2, 1)} & \text{if } \mu_1 = 1, \end{cases}$$

whilst for $\mu_2 \neq 0$,

$$\chi_2 \chi_{(\mu_1, \mu_2)} = \begin{cases} \chi_1 \chi_{(\mu_1, \mu_2)} + \chi_{(\mu_1, \mu_2)} + \chi_{(\mu_1-1, \mu_2-1)} + \chi_{(\mu_1+1, \mu_2+1)} \\ \quad + \chi_{(\mu_1+1, \mu_2-2)} + \chi_{(\mu_1-1, \mu_2+2)} + \chi_{(\mu_1+2, \mu_2-1)} + \chi_{(\mu_1-2, \mu_2+1)} & \text{if } \mu_1 \neq \mu_2, \mu_2 + 1, \\ \chi_{(\mu_1, \mu_1)} + \chi_{(\mu_1-1, \mu_1-1)} + \chi_{(\mu_1+1, \mu_1+1)} + \chi_{(\mu_1+1, \mu_1-1)} \\ \quad + \chi_{(\mu_1+1, \mu_1-2)} + \chi_{(\mu_1+2, \mu_1-1)} & \text{if } \mu_1 = \mu_2, \\ 2\chi_{(\mu_1, \mu_2)} + \chi_{(\mu_1-1, \mu_2-1)} + \chi_{(\mu_1+1, \mu_2+1)} + \chi_{(\mu_1+1, \mu_2-1)} \\ \quad + \chi_{(\mu_1+1, \mu_2-2)} + \chi_{(\mu_1+2, \mu_2-1)} + \chi_{(\mu_1+1, \mu_2)} + \chi_{(\mu_1, \mu_2-1)} & \text{if } \mu_1 = \mu_2 + 1, \end{cases}$$

where $\chi_{(\mu_1, \mu_2)} = 0$ if $\mu_2 < 0$ or $\mu_1 < \mu_2$.

Thus the McKay graph of G_2 for the first fundamental representation ρ_1 is identified with the infinite graph $\mathcal{A}_{\infty}^{\rho_1}(G_2)$, illustrated in Figure 5, where we have made a change of labeling to the Dynkin labels $(\lambda_1, \lambda_2) = (\mu_1 - \mu_2, \mu_2)$. This labeling is more convenient in order to be able to define self-adjoint operators v_N^1, v_N^2 in $\ell^2(\mathbb{N}) \otimes \ell^2(\mathbb{N})$ below. The dashed lines in Figure 5 indicate edges that are removed when one restricts to the graph $\mathcal{A}_k(G_2)$ at finite level k (here $k = 6$), c.f. Section 5.1.

Similarly, the McKay graph of G_2 for the second fundamental representation ρ_2 is identified with the infinite graph $\mathcal{A}_{\infty}^{\rho_2}(G_2)$, illustrated in Figure 6, again using the Dynkin labels $(\lambda_1, \lambda_2) = (\mu_1 - \mu_2, \mu_2)$, and where the dashed lines again indicate edges that are removed when one restricts to the graph $\mathcal{A}_k(G_2)$ at finite level k (here $k = 6$).

By [18, §3.5] we have $(\bigotimes_{\mathbb{N}} M_7)^{G_2} \cong A(\mathcal{A}_{\infty}^{\rho_1}(G_2))$ and $(\bigotimes_{\mathbb{N}} M_{14})^{G_2} \cong A(\mathcal{A}_{\infty}^{\rho_2}(G_2))$.

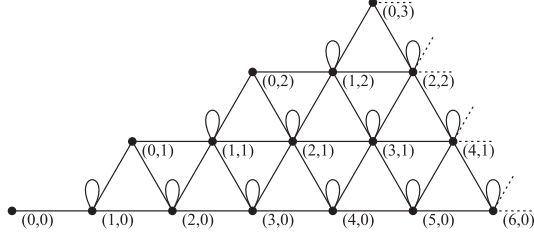


Figure 5: Infinite graph $\mathcal{A}_\infty^{\rho_1}(G_2)$

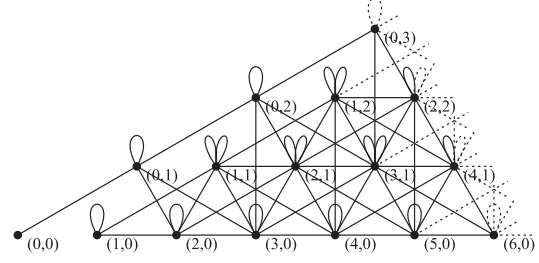


Figure 6: Infinite graph $\mathcal{A}_\infty^{\rho_2}(G_2)$

2.1 Spectral measures over different domains

The Weyl group W of G_2 is the dihedral group D_{12} of order 12. If we consider D_{12} as the subgroup of $GL(2, \mathbb{Z})$ generated by the matrices T_2, T_6 , of orders 2, 6 respectively, given by

$$T_2 = \begin{pmatrix} 0 & -1 \\ -1 & 0 \end{pmatrix}, \quad T_6 = \begin{pmatrix} 0 & 1 \\ -1 & 1 \end{pmatrix}, \quad (8)$$

then the action of D_{12} on \mathbb{T}^2 given by $T(\omega_1, \omega_2) = (\omega_1^{a_{11}} \omega_2^{a_{12}}, \omega_1^{a_{21}} \omega_2^{a_{22}})$, for $T = (a_{il}) \in D_{12}$, leaves $\chi_\mu(\omega_1, \omega_2)$ invariant, for any $\mu \in P_+$. Any D_{12} -invariant measure ε_μ on \mathbb{T}^2 yields a pushforward probability measure $\nu_\mu = (\chi_\mu)_*(\varepsilon_\mu)$ on $I_\mu = \chi_\mu(\mathbb{T}^2) \subset \mathbb{R}$ by

$$\int_{I_\mu} \psi(x) d\nu_\mu(x) = \int_{\mathbb{T}^2} \psi(\chi_\mu(\omega_1, \omega_2)) d\varepsilon_\mu(\omega_1, \omega_2), \quad (9)$$

for any continuous function $\psi : I_\mu \rightarrow \mathbb{C}$, where $d\varepsilon_\mu(\omega_1, \omega_2) = d\varepsilon_\mu(g(\omega_1, \omega_2))$ for all $g \in D_{12}$. There is a loss of dimension here, in the sense that the integral on the right hand side is over the two-dimensional torus \mathbb{T}^2 , whereas on the right hand side it is over the interval I_μ . Thus the preimage $I_\mu^{-1}[x]$ of any point x in the interior of I_μ is infinite, and there is an infinite family of pullback measures ε_μ over \mathbb{T}^2 for any measure ν_μ on I_μ , that is, any ε_μ such that $\varepsilon_\mu(I_\mu^{-1}[x]) = \nu_\mu(x)$ for all $x \in I_\mu$ will yield the probability measure ν_μ on I_μ as a pushforward measure by (9). We introduce below an intermediate probability measure $\tilde{\nu}_{\lambda, \mu}$ which lives over a (two-dimensional) subregion $\mathfrak{D}_{\lambda, \mu} \subset I_\lambda \times I_\mu \subset \mathbb{R}^2$, for $\lambda, \mu \in P_{++}$, for which there is a unique D_{12} -invariant measure $\varepsilon_{\lambda, \mu}$ on \mathbb{T}^2 . This measure $\tilde{\nu}_{\lambda, \mu}$ specializes to the spectral measures ν_λ, ν_μ of λ, μ respectively.

The permutation group S_3 appears as the subgroup generated by T_2 and the matrix $T_6^4 = -T_6$ of order 3 (c.f. [21, equation (37)]). Then D_{12} is generated by S_3 and the 2×2 matrix $-I$ which sends $\theta_l \leftrightarrow -\theta_l$, $l = 1, 2$. A fundamental domain of \mathbb{T}^2/D_{12} is thus given by a quotient of the fundamental domain of \mathbb{T}^2/S_3 , illustrated in Figure 7 (see [21]), by the \mathbb{Z}_2 -action given by the matrix $-I$. A fundamental domain F of \mathbb{T}^2 under the action of the dihedral group D_{12} is illustrated in Figure 8, where the axes are labelled by the parameters θ_1, θ_2 in $(e^{2\pi i \theta_1}, e^{2\pi i \theta_2}) \in \mathbb{T}^2$. In Figure 8, the lines $\theta_1 = 0$ and $\theta_2 = 0$ are also boundaries of copies of the fundamental domain F under the action of D_{12} , whereas they are not boundaries of copies of the fundamental domain under the action of S_3 in Figure 7. The torus \mathbb{T}^2 contains 12 copies of F , so that

$$\int_{\mathbb{T}^2} \phi(\omega_1, \omega_2) d\varepsilon_{\lambda, \mu}(\omega_1, \omega_2) = 12 \int_F \phi(\omega_1, \omega_2) d\varepsilon_{\lambda, \mu}(\omega_1, \omega_2), \quad (10)$$

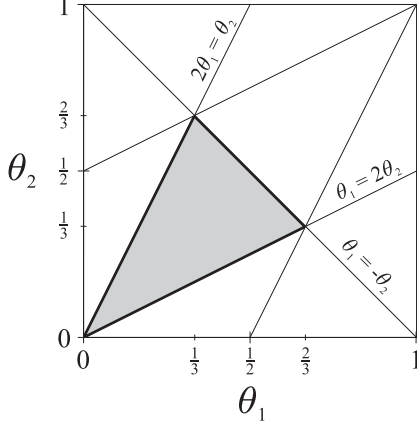


Figure 7: A fundamental domain of \mathbb{T}^2/S_3 .

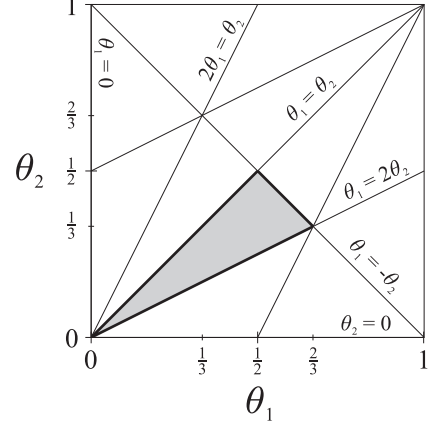


Figure 8: A fundamental domain F of \mathbb{T}^2/D_{12} .

for any D_{12} -invariant function $\phi : \mathbb{T}^2 \rightarrow \mathbb{C}$. The fixed points of \mathbb{T}^2 under the action of S_3 are the points $(1, 1)$, $(e^{2\pi i/3}, e^{4\pi i/3})$ and $(e^{4\pi i/3}, e^{2\pi i/3})$, but only the point $(1, 1)$ is fixed under the action of the whole of D_{12} . Under χ_{ρ_i} the point $(1, 1)$ maps to 7, 14 in the intervals I_{ρ_1} , I_{ρ_2} respectively, whilst the points $(e^{2\pi i/3}, e^{4\pi i/3})$, $(e^{4\pi i/3}, e^{2\pi i/3})$ both map to -2 (in both intervals).

Let $x_\lambda = \chi_\lambda(\omega_1, \omega_2)$ and let $\Psi_{\lambda, \mu}$ be the map $(\omega_1, \omega_2) \mapsto (x_\lambda, x_\mu)$. We denote by $\mathfrak{D}_{\lambda, \mu}$ the image of $\Psi_{\lambda, \mu}(F)$ ($= \Psi_{\lambda, \mu}(\mathbb{T}^2)$) in \mathbb{R}^2 . The joint spectral measure $\tilde{\nu}_{\lambda, \mu}$ is the measure on $\mathfrak{D}_{\lambda, \mu}$ uniquely determined by its cross-moments as in (1). Then there is a unique D_{12} -invariant pullback measure $\varepsilon_{\lambda, \mu}$ on \mathbb{T}^2 such that

$$\int_{\mathfrak{D}_{\lambda, \mu}} \psi(x_\lambda, x_\mu) d\tilde{\nu}_{\lambda, \mu}(x_\lambda, x_\mu) = \int_{\mathbb{T}^2} \psi(\chi_\lambda(\omega_1, \omega_2), \chi_\mu(\omega_1, \omega_2)) d\varepsilon_{\lambda, \mu}(\omega_1, \omega_2),$$

for any continuous function $\psi : \mathfrak{D}_{\lambda, \mu} \rightarrow \mathbb{C}$.

Any probability measure on $\mathfrak{D}_{\lambda, \mu}$ yields a probability measure on the interval I_λ , given by the pushforward $(p_\lambda)_*(\tilde{\nu}_{\lambda, \mu})$ of the joint spectral measure $\tilde{\nu}_{\lambda, \mu}$ under the orthogonal projection p_λ onto the spectrum $\sigma(\lambda)$. See [25, Section 2.5] for more details.

The following S_3 -invariant measures on \mathbb{T}^2 , defined in [22, Definition 1], will be useful later. Note that these measures are also invariant under D_{12} .

Definition 2.1. Let $\omega = e^{2\pi i/3}$, $\tau = e^{2\pi i/n}$. We define the following measures on \mathbb{T}^2 :

1. $d^{(n)}$, the uniform Dirac measure on the S_3 -orbit of the points (τ, τ) , $(\bar{\omega}\bar{\tau}, \omega)$, $(\omega, \bar{\omega}\bar{\tau})$, for $n \in \mathbb{Q}$, $n \geq 2$.
2. $d^{(n, k)}$, the uniform Dirac measure on the S_3 -orbit of the points $(\tau e^{2\pi i k}, \tau)$, $(\tau, \tau e^{2\pi i k})$, $(\bar{\omega}\bar{\tau}, \omega e^{2\pi i k})$, $(\omega e^{2\pi i k}, \bar{\omega}\bar{\tau})$, $(\bar{\omega}\bar{\tau} e^{-2\pi i k}, \omega e^{-2\pi i k})$, $(\omega e^{-2\pi i k}, \bar{\omega}\bar{\tau} e^{-2\pi i k})$, for $n, k \in \mathbb{Q}$, $n > 2$, $0 \leq k \leq 1/n$.

The sets $\text{Supp}(d^{(n)})$, $\text{Supp}(d^{(n, k)})$ are illustrated in [22, Figures 4, 5]. For $n > 2$ and $0 < k < 1/n$, $|\text{Supp}(d^{(n)})| = 18$, whilst $|\text{Supp}(d^{(n, k)})| = 36$. The cardinalities of the other sets are $|\text{Supp}(d^{(n, 0)})| = |\text{Supp}(d^{(n, 1/n)})| = 18$ for $n > 2$, and $|\text{Supp}(d^{((2))})| = 9$. Some relations between these measures are given in [22, Section 2].

3 Spectral measures for ${}^W\mathcal{A}_\infty(G_2)$

For the remainder of the paper we focus on the fundamental representations ρ_1 and ρ_2 of G_2 . We first consider their restrictions to \mathbb{T}^2 . As discussed in Section 2, their corresponding McKay graphs are ${}^W\mathcal{A}_\infty^{\rho_j}(G_2)$, illustrated in Figures 3, 4 for $j = 1, 2$ respectively.

We define commuting self-adjoint operators which may be identified with the adjacency matrix of ${}^W\mathcal{A}_\infty^{\rho_j}(G_2)$. We define operators v_Z^1, v_Z^2 on $\ell^2(\mathbb{Z}) \otimes \ell^2(\mathbb{Z})$ by

$$v_Z^1 = 1 \otimes 1 + s \otimes 1 + s^* \otimes 1 + 1 \otimes s + 1 \otimes s^* + s \otimes s^* + s^* \otimes s, \quad (11)$$

$$v_Z^2 = v_Z^1 + 1 \otimes 1 + s \otimes s + s^* \otimes s^* + s^2 \otimes s^* + (s^*)^2 \otimes s + s \otimes (s^*)^2 + s^* \otimes s^2, \quad (12)$$

where the unitary s is the bilateral shift on $\ell^2(\mathbb{Z})$. Let Ω denote the vector $(\delta_{i,0})_i$. Then v_Z^j is identified with the adjacency matrix of ${}^W\mathcal{A}_\infty^{\rho_j}(G_2)$, $j = 1, 2$, where we regard the vector $\Omega \otimes \Omega$ as corresponding to the vertex $(0, 0)$ of ${}^W\mathcal{A}_\infty^{\rho_j}(G_2)$, and the operators of the form $s^l \otimes s^m$ which appear as terms in v_Z^j as corresponding to the edges on ${}^W\mathcal{A}_\infty^{\rho_j}(G_2)$. Then $(s^{\lambda_1} \otimes s^{\lambda_2})(\Omega \otimes \Omega)$ corresponds to the vertex (λ_1, λ_2) of ${}^W\mathcal{A}_\infty^{\rho_j}(G_2)$ for any $\lambda_1, \lambda_2 \in \mathbb{Z}$, and applying $(v_Z^j)^m$ to $\Omega \otimes \Omega$ gives a vector $y = (y_{(\lambda_1, \lambda_2)})$ in $\ell^2({}^W\mathcal{A}_\infty^{\rho_j}(G_2))$, where $y_{(\lambda_1, \lambda_2)}$ gives the number of paths of length m on ${}^W\mathcal{A}_\infty^{\rho_j}(G_2)$ from $(0, 0)$ to the vertex (λ_1, λ_2) .

We define a state φ on $C^*(v_Z^1, v_Z^2)$ by $\varphi(\cdot) = \langle \cdot (\Omega \otimes \Omega), \Omega \otimes \Omega \rangle$. We use the notation $(a_1, a_2, \dots, a_k)!$ to denote the multinomial coefficient $(\sum_{i=1}^k a_i)! / \prod_{i=1}^k (a_i)!$. Then we have cross moments

$$\begin{aligned} s_{m,n} &= \varphi((v_Z^1)^m (v_Z^2)^n) \\ &= \sum_{\substack{k_i \geq 0 \\ \sum_i k_i \leq m}} \sum_{\substack{l_i \geq 0 \\ \sum_i l_i \leq n}} (k_1, k_2, \dots, k_6, m - \sum_i k_i)! (l_1, l_2, \dots, l_{12}, n - \sum_i l_i)! \varphi(s^{r_1} \otimes s^{r_2}) \\ &= \sum_{\substack{k_i \geq 0 \\ \sum_i k_i \leq m}} \sum_{\substack{l_i \geq 0 \\ \sum_i l_i \leq n}} (k_1, k_2, \dots, k_6, m - \sum_i k_i)! (l_1, l_2, \dots, l_{12}, n - \sum_i l_i)! \delta_{r_1,0} \delta_{r_2,0}, \end{aligned} \quad (13)$$

where

$$r_1 = k_1 - k_2 + k_5 - k_6 + l_1 - l_2 + l_5 - l_6 + l_7 - l_8 + 2l_9 - 2l_{10} + l_{11} - l_{12}, \quad (14)$$

$$r_2 = k_3 - k_4 - k_5 + k_6 + l_3 - l_4 - l_5 + l_6 + l_7 - l_8 - l_9 + l_{10} - 2l_{11} + 2l_{12}, \quad (15)$$

If $n = 0$ then $l_i = 0$ for all i , and we get a non-zero contribution when $k_4 = k_1 - k_2 + k_3$ and $k_6 = k_1 - k_2 + k_5$. So we obtain

$$\varphi((v_Z^1)^m) = \sum_{k_i} (k_1, k_2, k_3, k_1 - k_2 + k_3, k_5, k_1 - k_2 + k_5, m - 3k_1 + k_2 - 2k_3 - 2k_5)! \quad (16)$$

where the summation is over all integers $k_1, k_2, k_3, k_5 \geq 0$ such that $0 \leq k_1 - k_2 + k_3, k_1 - k_2 + k_5, 3k_1 - k_2 + 2k_3 + 2k_5 \leq m$. If $m = 0$ then $k_i = 0$ for all i , and we get a non-zero contribution when $l_4 = l_1 - l_2 + l_3 + 2l_7 - 2l_8 + l_9 - l_{10} - l_{11} + l_{12}$ and $l_6 = l_1 - l_2 + l_5 + l_7 - l_8 + 2l_9 - 2l_{10} + l_{11} - l_{12}$. So we obtain

$$\varphi((v_Z^2)^n) = \sum_{l_i} 2^{n-p_3} (l_1, l_2, l_3, p_1, l_5, p_2, l_7, l_8, l_9, l_{10}, l_{11}, l_{12}, n - p_3)! \quad (17)$$

where $p_1 = l_1 - l_2 + l_3 + 2l_7 - 2l_8 + l_9 - l_{10} - l_{11} + l_{12}$, $p_2 = l_1 - l_2 + l_5 + l_7 - l_8 + 2l_9 - 2l_{10} + l_{11} - l_{12}$, $p_3 = 3l_1 - l_2 + 2l_3 + 2l_5 + 4l_7 - 2l_8 + 4l_9 - 2l_{10} + l_{11} + l_{12}$ and the summation is over all integers $l_1, l_2, l_3, l_5, l_7, l_8, l_9, l_{10}, l_{11}, l_{12} \geq 0$ such that $0 \leq p_1, p_2, p_3 \leq n$.

3.1 Joint spectral measure for ${}^W\mathcal{A}_\infty(G_2)$ over \mathbb{T}^2

The ranges of the restrictions (5), (6) of the characters χ_j , $j = 1, 2$, of the fundamental representations of G_2 to \mathbb{T}^2 are given by I_j , where $I_1 := I_{\rho_1} = \{1 + 2\operatorname{Re}(\omega_1) + 2\operatorname{Re}(\omega_2) + 2\operatorname{Re}(\omega_1\omega_2^{-1}) \mid \omega_1, \omega_2 \in \mathbb{T}\} = [-2, 7]$ and $I_2 := I_{\rho_2} = \{2 + 2\operatorname{Re}(\omega_1) + 2\operatorname{Re}(\omega_2) + 2\operatorname{Re}(\omega_1\omega_2^{-1}) + 2\operatorname{Re}(\omega_1\omega_2) + 2\operatorname{Re}(\omega_1^2\omega_2^{-1}) + 2\operatorname{Re}(\omega_1\omega_2^{-2}) \mid \omega_1, \omega_2 \in \mathbb{T}\} = [-2, 14]$. Since the spectrum $\sigma(s)$ of s is \mathbb{T} , the spectrum $\sigma(v_Z^1)$ of v_Z^1 is $I_1 = [-2, 7]$, and the spectrum $\sigma(v_Z^2)$ of v_Z^2 is $I_2 = [-2, 14]$. We now determine the D_{12} -invariant spectral measure ε on \mathbb{T}^2 for the graphs ${}^W\mathcal{A}_\infty^{\rho_j}(G_2)$, $j = 1, 2$.

Theorem 3.1. *The joint spectral measure $\varepsilon(\omega_1, \omega_2)$ (on \mathbb{T}^2) for the graphs ${}^W\mathcal{A}_\infty^{\rho_j}(G_2)$, $j = 1, 2$, is given by the uniform Lebesgue measure $d\varepsilon(\omega_1, \omega_2) = d\omega_1 d\omega_2$.*

Proof: The m, n^{th} cross moment is given by

$$\begin{aligned} & \int_{\mathbb{T}^2} (\chi_1(\omega_1, \omega_2))^m (\chi_2(\omega_1, \omega_2))^n d\omega_1 d\omega_2 \\ &= \sum_{\substack{k_i \geq 0 \\ \sum_i k_i \leq m}} \sum_{\substack{l_i \geq 0 \\ \sum_i l_i \leq n}} (k_1, k_2, \dots, k_6, m - \sum_i k_i)! (l_1, l_2, \dots, l_{12}, n - \sum_i l_i)! \int_{\mathbb{T}^2} \omega_1^{r_1} \omega_2^{r_2} d\omega_1 d\omega_2 \\ &= \sum_{\substack{k_i \geq 0 \\ \sum_i k_i \leq m}} \sum_{\substack{l_i \geq 0 \\ \sum_i l_i \leq n}} (k_1, k_2, \dots, k_6, m - \sum_i k_i)! (l_1, l_2, \dots, l_{12}, n - \sum_i l_i)! \delta_{r_1, 0} \delta_{r_2, 0}, \end{aligned}$$

where r_1, r_2 are as in (14), (15), since $\int_{\mathbb{T}} u^m du = \delta_{m, 0}$. This is equal to the cross moments $\varphi((v_Z^1)^m (v_Z^2)^n)$ given in (13). \square

In fact, the measure $\varepsilon(\omega_1, \omega_2)$ given above is the joint spectral measure over \mathbb{T}^2 for the pair of McKay graphs $({}^W\mathcal{A}_\infty^\lambda(G_2), {}^W\mathcal{A}_\infty^\mu(G_2))$ for any pair λ, μ of irreducible representations of G_2 , by a similar proof. Thus the spectral measure over \mathbb{T}^2 is independent of the choice of irreducible representations used to construct the McKay graphs.

3.2 Joint spectral measure for ${}^W\mathcal{A}_\infty(G_2)$ on \mathfrak{D}

Let $x := x_{(1,0)} = \chi_1(\omega_1, \omega_2)$ and $y := x_{(1,1)} = \chi_2(\omega_1, \omega_2)$, or explicitly,

$$x = 1 + 2 \cos(2\pi\theta_1) + 2 \cos(2\pi\theta_2) + 2 \cos(2\pi(\theta_1 - \theta_2)), \quad (18)$$

$$y = x + 1 + 2 \cos(2\pi(\theta_1 + \theta_2)) + 2 \cos(2\pi(2\theta_1 - \theta_2)) + 2 \cos(2\pi(\theta_1 - 2\theta_2)), \quad (19)$$

and denote by Ψ the map $\Psi_{(1,0),(1,1)} : (\omega_1, \omega_2) \mapsto (x, y)$.

We now describe $\mathfrak{D} := \mathfrak{D}_{(1,0),(1,1)}$, illustrated in Figure 9, which is the joint spectrum $\sigma(v_Z^1, v_Z^2)$ of the commuting self-adjoint operators v_Z^1, v_Z^2 . The boundary of F given by $\theta_1 = 2\theta_2$ yields the curves c_1, c_2 for $\theta_2 \in [0, 1/3]$, which are both given by the parametric equations

$$\begin{aligned} x &= 1 + 4 \cos(2\pi\theta_2) + 2 \cos(4\pi\theta_2) = -1 + 4 \cos(2\pi\theta_2) + 4 \cos^2(2\pi\theta_2), \\ y &= 4 + 4 \cos(2\pi\theta_2) + 2 \cos(4\pi\theta_2) + 4 \cos(6\pi\theta_2) \\ &= 2 - 8 \cos(2\pi\theta_2) + 4 \cos^2(2\pi\theta_2) + 16 \cos^3(2\pi\theta_2). \end{aligned}$$

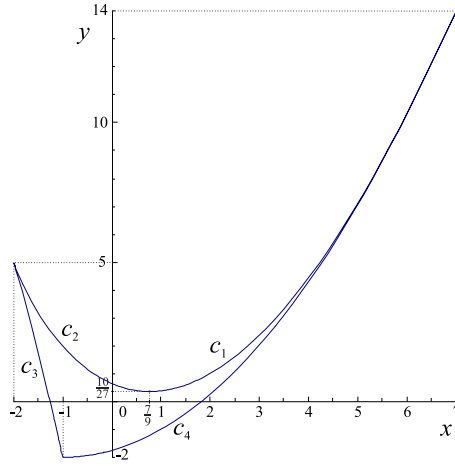


Figure 9: The domain $\mathfrak{D} = \Psi(F)$ for G_2 .

The boundary of F given by $\theta_1 = -\theta_2$ yields the curve c_3 given by the parametric equations

$$\begin{aligned} x &= -1 + 4 \cos(2\pi\theta_1) + 4 \cos^2(2\pi\theta_1), \\ y &= 2 - 8 \cos(2\pi\theta_1) + 4 \cos^2(2\pi\theta_1) + 16 \cos^3(2\pi\theta_1), \end{aligned}$$

where $\theta_1 \in [1/2, 2/3]$. Finally, the boundary $\theta_1 = \theta_2$ of F yields the curve c_4 given by the parametric equations

$$\begin{aligned} x &= 3 + 4 \cos(2\pi\theta_1), \\ y &= 4 + 8 \cos(2\pi\theta_1) + 2 \cos(4\pi\theta_1) = 2 + 8 \cos(2\pi\theta_1) + 4 \cos^2(2\pi\theta_1), \end{aligned}$$

where $\theta_1 \in [1/2, 1]$. As functions of x , the boundaries of \mathfrak{D} are obtained by writing $\cos(2\pi\theta)$ in terms of x in the above parametric equations, which are at worst quadratic in $\cos(2\pi\theta)$. The boundaries of \mathfrak{D} are thus given by the curves [40]

$$c_1 : \quad y = -5(x+1) + 2(x+2)^{3/2}, \quad x \in [-2, 7/9], \quad (20)$$

$$c_2 : \quad y = -5(x+1) + 2(x+2)^{3/2}, \quad x \in [7/9, 7], \quad (21)$$

$$c_3 : \quad y = -5(x+1) - 2(x+2)^{3/2}, \quad x \in [-2, -1], \quad (22)$$

$$c_4 : \quad 4y = x^2 + 2x - 7, \quad x \in [-1, 7]. \quad (23)$$

On the other hand, writing these curves as function of y involves cubic equations in $\cos(2\pi\theta)$, and the boundaries of \mathfrak{D} are given by the curves

$$c_1 : \quad x = -1 + 4p_2(y) + 4p_2(y)^2, \quad y \in [10/27, 14], \quad (24)$$

$$c_2 : \quad x = -1 + 4p_3(y) + 4p_3(y)^2, \quad y \in [10/27, 5] \quad (25)$$

$$c_3 : \quad x = -1 + 4p_1(y) + 4p_1(y)^2, \quad y \in [-2, 5], \quad (26)$$

$$c_4 : \quad x = -1 + 2(y+2)^{1/2}, \quad y \in [-2, 14], \quad (27)$$

where p_i is given by $12p_i(y) = -1 - \epsilon_i P - 25\overline{\epsilon_i} P^{-1}$, for $\epsilon_j = e^{2\pi i(j-1)/3}$ and $P = (145 - 54y + 2\sqrt{3^3(27y^2 - 145y + 50)})^{1/3}$, and we take the positive square root in equation (27).

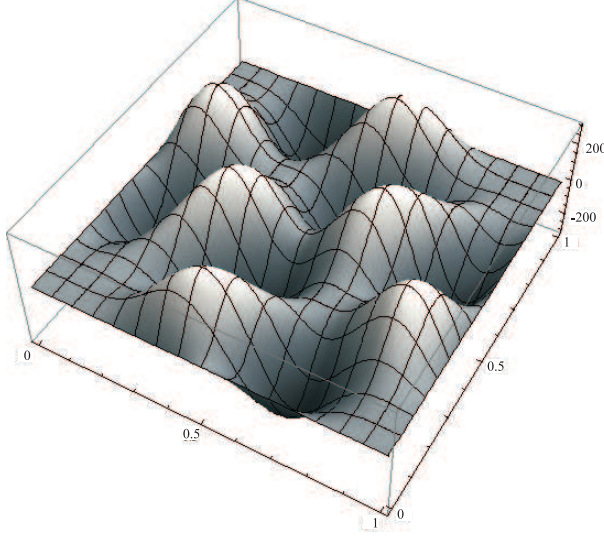


Figure 10: The Jacobian J over \mathbb{T}^2 .

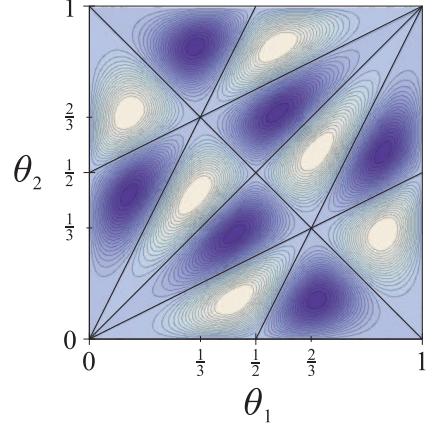


Figure 11: Contour plot of J over \mathbb{T}^2 .

Under the change of variables (18), (19), the Jacobian $J = \det(\partial(x, y)/\partial(\theta_1, \theta_2))$ is given by

$$J(\theta_1, \theta_2) = 8\pi^2(\cos(2\pi(2\theta_1 + \theta_2)) + \cos(2\pi(\theta_1 - 3\theta_2)) + \cos(2\pi(3\theta_1 - 2\theta_2)) - \cos(2\pi(\theta_1 + 2\theta_2)) - \cos(2\pi(3\theta_1 - \theta_2)) - \cos(2\pi(2\theta_1 - 3\theta_2))). \quad (28)$$

The Jacobian is real and is illustrated in Figures 10, 11, where its values are plotted over the torus \mathbb{T}^2 .

With $\omega_j = e^{2\pi i \theta_j}$, $j = 1, 2$, the Jacobian is given in terms of $\omega_1, \omega_2 \in \mathbb{T}$ by

$$\begin{aligned} J(\omega_1, \omega_2) &= 8\pi^2 \text{Re}(\omega_1^2 \omega_2 + \omega_1 \omega_2^{-3} + \omega_1^3 \omega_2^{-2} - \omega_1 \omega_2^2 - \omega_1^3 \omega_2^{-1} - \omega_1^2 \omega_2^{-3}) \\ &= 4\pi^2(\omega_1^2 \omega_2 + \omega_1^{-2} \omega_2^{-1} + \omega_1 \omega_2^{-3} + \omega_1^{-1} \omega_2^3 + \omega_1^3 \omega_2^{-2} + \omega_1^{-3} \omega_2^2 \\ &\quad - \omega_1 \omega_2^2 - \omega_1^{-1} \omega_2^{-2} - \omega_1^3 \omega_2^{-1} - \omega_1^{-3} \omega_2 - \omega_1^2 \omega_2^{-3} - \omega_1^{-2} \omega_2^3). \end{aligned} \quad (29)$$

The Jacobian J is invariant under $T_6 \in D_{12}$, whilst $T_2(J) = -J$. Thus J^2 is invariant under the action of D_{12} , and we seek an expression for J^2 in terms of the D_{12} -invariant variables x, y , which may be obtained as a product of the roots appearing as the equations of the boundary of \mathfrak{D} in (20)-(23), and is given (up to a factor of $16\pi^4$) as (see also [40])

$$J^2(x, y) = (4x^3 - x^2 - 2x - 10xy - y^2 - 10y + 7)(x^2 + 2x - 7 - 4y), \quad (30)$$

for $(x, y) \in \mathfrak{D}$, which can easily be checked by substituting for x, y as in (18), (19). Note that the Jacobian (30) is a cubic in y , with the three roots appearing as the equations of the boundary of \mathfrak{D} in (20)-(23). However, although the Jacobian (30) is a quintic in x , only four of the roots appear as the equations of the boundary of \mathfrak{D} in (24)-(27). The fifth root $x = -1 - 2(y + 2)^{1/2}$ only intersects with \mathfrak{D} at the point $(-1, -2)$. The factorization of J in (30) and the equations for the boundaries of \mathfrak{D} given in (20)-(27) will be used in Sections 3.3, 4.2 to determine explicit expressions for the weights which appear in the spectral measures $\mu_{v_Z^j}$ over I_j in terms of elliptic integrals. From (30) we see that the

Jacobian vanishes only on the boundary of \mathfrak{D} , or over \mathbb{T}^2 only on the boundaries of the images of the fundamental domain F under D_{12} .

Since J is real, $J^2 \geq 0$, and we have the following expressions for the Jacobian J :

$$\begin{aligned} J(\theta_1, \theta_2) &= 8\pi^2(\cos(2\pi(2\theta_1 + \theta_2)) + \cos(2\pi(\theta_1 - 3\theta_2)) + \cos(2\pi(3\theta_1 - 2\theta_2)) \\ &\quad - \cos(2\pi(\theta_1 + 2\theta_2)) - \cos(2\pi(3\theta_1 - \theta_2)) - \cos(2\pi(2\theta_1 - 3\theta_2))), \\ J(\omega_1, \omega_2) &= 4\pi^2(\omega_1^2\omega_2 + \omega_1^{-2}\omega_2^{-1} + \omega_1\omega_2^{-3} + \omega_1^{-1}\omega_2^3 + \omega_1^3\omega_2^{-2} + \omega_1^{-3}\omega_2^2 \\ &\quad - \omega_1\omega_2^2 - \omega_1^{-1}\omega_2^{-2} - \omega_1^3\omega_2^{-1} - \omega_1^{-3}\omega_2 - \omega_1^2\omega_2^{-3} - \omega_1^{-2}\omega_2^3), \\ |J(x, y)| &= 4\pi^2\sqrt{(4x^3 - x^2 - 2x - 10xy - y^2 - 10y + 7)(x^2 + 2x - 7 - 4y)}, \end{aligned}$$

where $0 \leq \theta_1, \theta_2 < 1$, $\omega_1, \omega_2 \in \mathbb{T}$ and $(x, y) \in \mathfrak{D}$. Note that the expression under the square root is real and non-negative since J^2 is.

Then

$$\int_F \psi(\chi_1(\omega_1, \omega_2), \chi_2(\omega_1, \omega_2)) d\omega_1 d\omega_2 = \int_{\mathfrak{D}} \psi(x, y) |J(x, y)|^{-1} dx dy, \quad (31)$$

and from Theorem 3.1 and (10) we obtain

Theorem 3.2. *The joint spectral measure $\tilde{\nu}$ (over \mathfrak{D}) for the graphs $W\mathcal{A}_{\infty}^{\rho_j}(G_2)$, $j = 1, 2$, is*

$$d\tilde{\nu}(x, y) = 12 |J(x, y)|^{-1} dx dy.$$

3.3 Spectral measure for $W\mathcal{A}_{\infty}(G_2)$ on \mathbb{R}

We now compute the spectral measure $\nu_{v_Z^j} = \nu_{\rho_j}$ over I_j , which is determined by its moments $\varphi((v_Z^j)^m) = \int_{I_j} x_j^m d\nu_{v_Z^j}(x_j)$ for all $m \in \mathbb{N}$, where $x_j = x, y$ for $j = 1, 2$ respectively.

For $\nu_{v_Z^1}$ we set $\psi(x, y) = x^m$ in (31) and integrate with respect to y . Similarly, setting $\psi(x, y) = y^m$ in (31), the measure $\nu_{v_Z^2}$ is obtained by integrating with respect to x . More explicitly, using the expressions for the boundaries of \mathfrak{D} given in (20)-(27), the spectral measure $\nu_{v_Z^1}$ (over $[-2, 7]$) for the graph $W\mathcal{A}_{\infty}^{\rho_1}(G_2)$ is $d\nu_{v_Z^1}(x) = J_1^{\mathbb{T}^2}(x) dx$, where $J_1^{\mathbb{T}^2}(x)$ is given by

$$J_1^{\mathbb{T}^2}(x) = \begin{cases} 12 \int_{-5(x+1)-2(x+2)^{3/2}}^{-5(x+1)+2(x+2)^{3/2}} |J(x, y)|^{-1} dy & \text{for } x \in [-2, -1], \\ 12 \int_{(x^2+2x-7)/4}^{-5(x+1)+2(x+2)^{3/2}} |J(x, y)|^{-1} dy & \text{for } x \in [-1, 7]. \end{cases}$$

The weight $J_1^{\mathbb{T}^2}(x)$ is an integral of the reciprocal of the square root of a cubic in y , and thus can be written in terms of the complete elliptic integral $K(m)$ of the first kind, $K(m) = \int_0^{\pi/2} (1 - m \sin^2 \theta)^{-1/2} d\theta$. Using [10, Eqn. 235.00],

$$\frac{6}{\pi^2 (8(x+2)^{3/2} - x^2 - 22x - 13)^{1/2}} K(v(x)) = \frac{3v(x)^{1/2}}{2\pi^2 (x+2)^{3/4}} K(v(x))$$

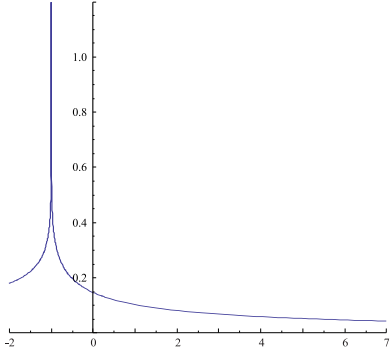


Figure 12: $J_1^{\mathbb{T}^2}(x)$

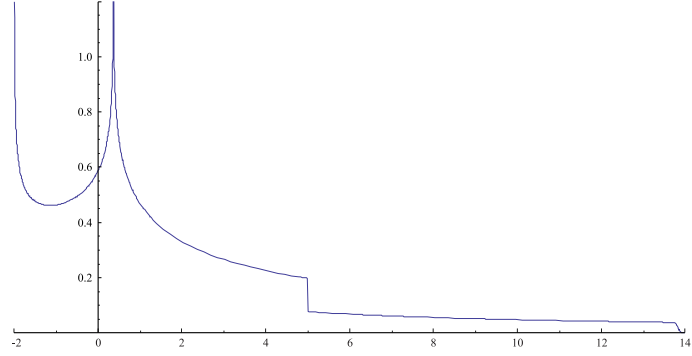


Figure 13: $J_2^{\mathbb{T}^2}(y)$

for $x \in [-2, -1]$, where $v(x) = 16(x+2)^{3/2}/(8(x+2)^{3/2} - x^2 - 22x - 13)$, whilst for $x \in [-1, 7]$,

$$\frac{6v(x)^{-1/2}}{\pi^2(8(x+2)^{3/2} - x^2 - 22x - 13)^{1/2}} K(v(x)^{-1}) = \frac{3}{2\pi^2(x+2)^{3/4}} K(v(x)^{-1}).$$

The weight $J_1^{\mathbb{T}^2}(x)$ is illustrated in Figure 12, up to a factor $4\pi^2$.

The spectral measure $\nu_{v_Z^2}$ (over $[-2, 14]$) for the graph $^W\mathcal{A}_\infty^{\rho_2}(G_2)$ is $d\nu_{v_Z^2}(y) = J_2^{\mathbb{T}^2}(y) dy$, where $J_2^{\mathbb{T}^2}(y)$ is given by

$$\begin{aligned} & 12 \int_{-1+4p_1(y)+4p_1(y)^2}^{-1+2(y+2)^{1/2}} |J(x, y)|^{-1} dx && \text{for } y \in [-2, 10/27], \\ & 12 \int_{-1+4p_1(y)+4p_1(y)^2}^{-1+4p_3(y)+4p_3(y)^2} |J(x, y)|^{-1} dx + 12 \int_{-1+4p_2(y)+4p_2(y)^2}^{-1+2(y+2)^{1/2}} |J(x, y)|^{-1} dx && \text{for } y \in [10/27, 5], \\ & 12 \int_{-1+4p_2(y)+4p_2(y)^2}^{-1+2(y+2)^{1/2}} |J(x, y)|^{-1} dx && \text{for } y \in [5, 14]. \end{aligned}$$

A numerical plot of the weight $J_2^{\mathbb{T}^2}(y)$ is illustrated in Figure 13, again up to a factor $4\pi^2$.

4 Spectral measures for $\mathcal{A}_\infty(G_2)$

We now consider the fundamental representations ρ_j , $j = 1, 2$, of G_2 . As discussed in Section 2, their corresponding McKay graphs are $\mathcal{A}_\infty^{\rho_j}(G_2)$, $j = 1, 2$. This section follows the same arguments as [21, §6.2]. The new feature here is the presence of terms such as $l^m(l^*)^p$ for $m \leq p$, where l is the unilateral shift to the right on $\ell^2(\mathbb{N})$, which correspond to the fact that certain edges on the graphs $\mathcal{A}_\infty^{\rho_j}(G_2)$, $j = 1, 2$, only appear when far enough away from the boundary of the graph.

We define self-adjoint operators v_N^1, v_N^2 on $\ell^2(\mathbb{N}) \otimes \ell^2(\mathbb{N})$ by

$$v_N^1 = ll^* \otimes 1 + l \otimes 1 + l^* \otimes 1 + l^* \otimes l + l \otimes l^* + l^2 \otimes l^* + (l^*)^2 \otimes l, \quad (32)$$

$$\begin{aligned} v_N^2 = & ll^* \otimes 1 + l^2 l^* \otimes 1 + l(l^*)^2 \otimes 1 + l(l^*)^2 \otimes l + l^2 l^* \otimes l^* + l^2 \otimes l^* + (l^*)^2 \otimes l \\ & + 1 \otimes ll^* + 1 \otimes l + 1 \otimes l^* + l^3 \otimes l^* + (l^*)^3 \otimes l + l^3 \otimes (l^*)^2 + (l^*)^3 \otimes l^2. \end{aligned} \quad (33)$$

Let Ω denote the vector $(\delta_{i,0})_i$. Then v_N^j is identified with the adjacency matrix of $\mathcal{A}_\infty^{\rho_j}(G_2)$, $j = 1, 2$, where we regard the vector $\Omega \otimes \Omega$ as corresponding to the vertex $(0, 0)$ of $\mathcal{A}_\infty^{\rho_j}(G_2)$, and the operators of the form $l^{m_1}(l^*)^{p_1} \otimes l^{m_2}(l^*)^{p_2}$ which appear as terms in v_N^j as corresponding to the edges on $\mathcal{A}_\infty^{\rho_j}(G_2)$. Then $(l^{\lambda_1} \otimes l^{\lambda_2})(\Omega \otimes \Omega)$ corresponds to the vertex (λ_1, λ_2) of $\mathcal{A}_\infty^{\rho_j}(G_2)$ for any $\lambda_1, \lambda_2 \in \mathbb{N}$, and applying $(v_N^j)^m$ to $\Omega \otimes \Omega$ gives a vector $y = (y_{(\lambda_1, \lambda_2)})$ in $\ell^2(\mathcal{A}_\infty^{\rho_j}(G_2))$, where $y_{(\lambda_1, \lambda_2)}$ gives the number of paths of length m on $\mathcal{A}_\infty^{\rho_j}(G_2)$ from $(0, 0)$ to the vertex (λ_1, λ_2) . A term of the form $(l^m(l^*)^p \otimes 1)(\lambda_1, \lambda_2)$, $m < p$, will be zero if $\lambda_1 < p$. Thus for example, $(l^* \otimes 1)(0, \lambda_2) = 0$, which corresponds to the fact that there is no self-loop at the point $(0, \lambda_2)$ for any $\lambda_2 \in \mathbb{N}$, whereas $(l^* \otimes 1)(\lambda_1, \lambda_2) = (\lambda_1, \lambda_2)$ for all $\lambda_1 \neq 0$, corresponding to the fact that there is a self-loop at these points.

It is not immediately obvious that these two operators commute. However this can be easily seen from the fact that $\mathcal{A}_\infty^{\rho_j}(G_2)$ are the multiplication graphs for the characters χ_j of the fundamental representations ρ_j , $j = 1, 2$, of G_2 , where the vertices of $\mathcal{A}_\infty^{\rho_j}(G_2)$ are labeled by the characters of the irreducible representations of G_2 .

Any vector $l^{p_1}\Omega \otimes l^{p_2}\Omega \in \ell^2(\mathbb{N}) \otimes \ell^2(\mathbb{N})$ can be written as a linear combination of elements of the form $(v_N^1)^{m_1}(v_N^2)^{m_2}(\Omega \otimes \Omega)$. This is not obvious from the definition of the operators v_N^j given in (32), (33). However this also can be seen from the fact that $\mathcal{A}_\infty^{\rho_j}(G_2)$ are the multiplication graphs for the characters of the fundamental representations of G_2 , where $\Omega \otimes \Omega$ corresponds to the character $\chi_{(0,0)}$ of the trivial representation. The characters of all other irreducible representations can be written as a linear combination of products of the form $\chi_1^m \chi_2^n \chi_{(0,0)}$, which follows from [33, Proposition 1] where $X_1 = \chi_1 - \chi_{(0,0)}$ and $X_2 = \chi_2 - \chi_1 - \chi_{(0,0)}$.

Thus the vector $\Omega \otimes \Omega$ is cyclic in $\ell^2(\mathbb{N}) \otimes \ell^2(\mathbb{N})$, and we have $\overline{C^*(v_N^1, v_N^2)(\Omega \otimes \Omega)} = \ell^2(\mathbb{N}) \otimes \ell^2(\mathbb{N})$. We define a state φ on $C^*(v_N^1, v_N^2)$ by $\varphi(\cdot) = \langle \cdot (\Omega \otimes \Omega), \Omega \otimes \Omega \rangle$. Since $C^*(v_N^1, v_N^2)$ is abelian and $\Omega \otimes \Omega$ is cyclic, we have that φ is a faithful state on $C^*(v_N^1, v_N^2)$. Then by [42, Remark 2.3.2] the support of $\tilde{\nu}_{v_N^1, v_N^2}$ is equal to the joint spectrum $\sigma(v_N^1, v_N^2)$ of v_N^1, v_N^2 .

Recall the decompositions of $\chi_1 \chi_\mu$ and $\chi_2 \chi_\mu$ for the characters of G_2 given in Section 2. These can be written as $\chi_j \chi_\mu = \sum_\nu \Delta_{\rho_j}(\mu, \nu) \chi_\nu$, where Δ_{ρ_j} is the adjacency matrix of $\mathcal{A}_\infty^{\rho_j}(G_2)$, the McKay graph for the fundamental representation ρ_j of G_2 . This equation can be interpreted as meaning that v_N^j (identified with the adjacency matrix Δ_{ρ_j} of $\mathcal{A}_\infty^{\rho_j}(G_2)$) has eigenvector $(\chi_\nu(\theta))_\nu$ for eigenvalue $\chi_j(\theta)$, $\theta \in [0, 2\pi]^2$. Thus the spectrum of v_N^j is given by $\chi_j(\mathbb{T}^2)$, and the joint spectrum $\sigma(v_N^1, v_N^2)$ is \mathfrak{D} . The moments $\varphi((v_N^j)^m)$ count the number of closed paths of length m on the graph $\mathcal{A}_\infty^{\rho_j}(G_2)$ which start and end at the apex vertex $(0, 0)$.

4.1 Joint spectral measure for $\mathcal{A}_\infty(G_2)$ over \mathbb{T}^2

We prove in Section 5.1 that the measure given by $d\varepsilon(\omega_1, \omega_2) = J(\omega_1, \omega_2)^2 d\omega_1 d\omega_2 / 192\pi^4$ is the joint spectral measure over \mathbb{T}^2 of v_N^j , $j = 1, 2$, where $d\omega_l$ is the uniform Lebesgue measure on \mathbb{T} , $l = 1, 2$. In fact, the measure $\varepsilon(\omega_1, \omega_2)$ is the joint spectral measure over \mathbb{T}^2 for the pair of McKay graphs $(\mathcal{A}_\infty^\lambda(G_2), \mathcal{A}_\infty^\mu(G_2))$ for any pair λ, μ of irreducible representations of G_2 . We see that ε is (up to some scalar) the reduced Haar measure of G_2 (c.f. [40, §6.3]).

4.2 Spectral measure for $\mathcal{A}_\infty(G_2)$ on \mathbb{R}

We now determine the spectral measure $\nu_{v_N^j}$ over I_j . From (10) and (31), with the measure given in Section 4.1, we have that

$$\frac{1}{192\pi^4} \int_{\mathbb{T}^2} \psi(\chi_j(\omega_1, \omega_2)) J(\omega_1, \omega_2)^2 d\omega_1 d\omega_2 = \frac{1}{16\pi^4} \int_{\mathfrak{D}} \psi(x') |J(x, y)| dx dy, \quad (34)$$

where \mathfrak{D} is as in Section 3.2, and $x' = x, y$ for $j = 1, 2$ respectively. Thus the joint spectral measure over \mathfrak{D} is $|J(x, y)| dx dy / 16\pi^4$, which is the reduced Haar measure on G_2 [40, §6.3]. The measure $\nu_{v_N^1}$ over I_1 is obtained by integrating with respect to y in (34), whilst the measure $\nu_{v_N^2}$ over I_2 is obtained by integrating with respect to x in (34). More explicitly, using the expressions for the boundaries of \mathfrak{D} given in (20)-(27), the spectral measure $\nu_{v_N^1}$ (over $[-2, 7]$) for the graph $\mathcal{A}_\infty^{\rho_1}(G_2)$ is $d\nu_{v_N^1}(x) = J_1^{G_2}(x) dx / 16\pi^4$, where $J_1^{G_2}(x)$ is given by

$$J_1^{G_2}(x) = \begin{cases} \int_{-5(x+1)+2(x+2)^{3/2}}^{-5(x+1)-2(x+2)^{3/2}} |J(x, y)| dy & \text{for } x \in [-2, -1], \\ \int_{(x^2+2x-7)/4}^{-5(x+1)+2(x+2)^{3/2}} |J(x, y)| dy & \text{for } x \in [-1, 7]. \end{cases}$$

The weight $J_1^{G_2}(x)$ is the integral of the square root of a cubic in y , and thus can be written in terms of the complete elliptic integrals $K(m)$, $E(m)$ of the first, second kind respectively, where $K(m) = \int_0^{\pi/2} (1 - m \sin^2 \theta)^{-1/2} d\theta$ and $E(m) = \int_0^{\pi/2} (1 - m \sin^2 \theta)^{1/2} d\theta$. Using [10, equation 235.14], $J_1^{G_2}(x)$ is given by

$$\frac{\pi^2}{15} (8(x+2)^{3/2} - x^2 - 22x - 13)^{1/2} \left[(x^4 + 236x^3 + 1662x^2 + 2876x + 1705) E(v(x)) - (8(x+2)^{3/2} + x^2 + 22x + 13)(x^2 + 22x + 13) K(v(x)) \right],$$

for $x \in [-2, -1]$, where $v(x) = 16(x+2)^{3/2} / (8(x+2)^{3/2} - x^2 - 22x - 13)$, whilst for $x \in [-1, 7]$, $J_1^{G_2}(x)$ is given by

$$\frac{2\pi^2}{15} (x+2)^{3/4} \left[2(x^4 + 236x^3 + 1662x^2 + 2876x + 1705) E(v(x)^{-1}) - (8(x+2)^{3/2} + x^2 + 22x + 13)(24(x+2)^{3/2} + x^2 + 22x + 13) K(v(x)^{-1}) \right].$$

The weight $J_1^{G_2}(x)$ is illustrated in Figure 14, up to a factor $4\pi^2$.

The spectral measure $\nu_{v_N^2}$ (over $[-2, 14]$) for the graph $\mathcal{A}_\infty^{\rho_2}(G_2)$ is $d\nu_{v_N^2}(y) = J_2^{G_2}(y) dy / 16\pi^4$, where $J_2^{G_2}(y)$ is given by

$$\begin{aligned} & \int_{-1+4p_1(y)+4p_1(y)^2}^{-1+2(y+2)^{1/2}} |J(x, y)| dx && \text{for } y \in [-2, 10/27], \\ & \int_{-1+4p_1(y)+4p_1(y)^2}^{-1+4p_3(y)+4p_3(y)^2} |J(x, y)| dx + \int_{-1+4p_2(y)+4p_2(y)^2}^{-1+2(y+2)^{1/2}} |J(x, y)| dx && \text{for } y \in [10/27, 5], \\ & \int_{-1+4p_2(y)+4p_2(y)^2}^{-1+2(y+2)^{1/2}} |J(x, y)| dx && \text{for } y \in [5, 14]. \end{aligned}$$

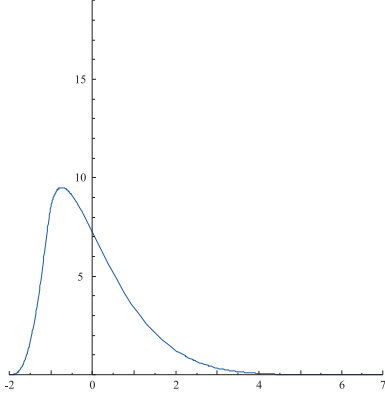


Figure 14: $J_1^{G_2}(x)$

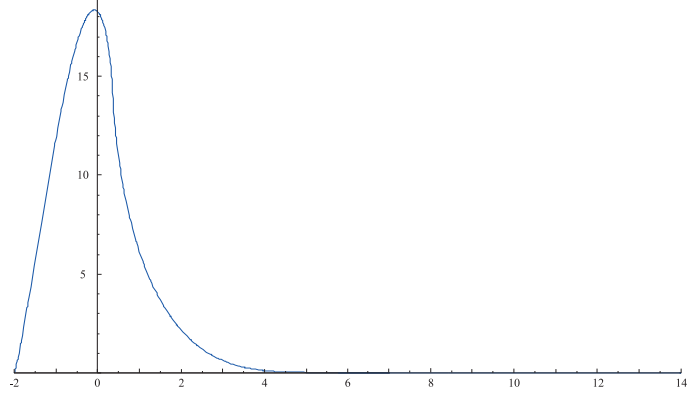


Figure 15: $J_2^{G_2}(y)$

A numerical plot of the weight $J_2^{G_2}(y)$ is illustrated in Figure 15, again up to a factor $4\pi^2$.

5 Joint spectral measures for nimrep graphs associated to G_2 modular invariants

Suppose G is the nimrep associated to a G_2 braided subfactor at some finite level k with vertex set G_0 . We define a state φ on $\ell^2(G_0)$ by $\varphi(\cdot) = \langle \cdot, \Omega \rangle$, where Ω is the basis vector in $\ell^2(G_0)$ corresponding to a distinguished vertex $*$. Note that the state φ (and thus the spectral measure) depends on the choice of distinguished vertex $*$. We choose the distinguished vertex $*$ to be the vertex with lowest Perron-Frobenius weight.

Consider the nimrep graph G_λ . The eigenvalues $\beta_\lambda^{(\mu)}$ of G_λ are given by the ratio $S_{\lambda,\mu}/S_{0,\mu}$, where μ belongs to the set $\text{Exp}(G)$ of exponents of G , $\text{Exp}(G) \subset P_+^k = \{(\lambda_1, \lambda_2) \mid \lambda_1, \lambda_2 \geq 0; \lambda_1 + 2\lambda_2 \leq k\}$ (note that we are now using the Dynkin labels), and the S -matrix at level k is given by [32, 26]:

$$S_{\lambda,\mu} = \frac{-2}{(k+4)\sqrt{3}} \left[\begin{aligned} &\cos(2\xi(2(\hat{\lambda}_1 + \hat{\lambda}_2)(\hat{\mu}_1 + \hat{\mu}_2) + (\hat{\lambda}_1 + \hat{\lambda}_2)\hat{\mu}_2 + \hat{\lambda}_2(\hat{\mu}_1 + \hat{\mu}_2) + 2\hat{\lambda}_2\hat{\mu}_2)) \\ &+ \cos(2\xi(-(\hat{\lambda}_1 + \hat{\lambda}_2)(\hat{\mu}_1 + \hat{\mu}_2) - 2(\hat{\lambda}_1 + \hat{\lambda}_2)\hat{\mu}_2 + \hat{\lambda}_2(\hat{\mu}_1 + \hat{\mu}_2) - \hat{\lambda}_2\hat{\mu}_2)) \\ &+ \cos(2\xi(-(\hat{\lambda}_1 + \hat{\lambda}_2)(\hat{\mu}_1 + \hat{\mu}_2) + (\hat{\lambda}_1 + \hat{\lambda}_2)\hat{\mu}_2 - 2\hat{\lambda}_2(\hat{\mu}_1 + \hat{\mu}_2) - \hat{\lambda}_2\hat{\mu}_2)) \\ &- \cos(2\xi(-(\hat{\lambda}_1 + \hat{\lambda}_2)(\hat{\mu}_1 + \hat{\mu}_2) - 2(\hat{\lambda}_1 + \hat{\lambda}_2)\hat{\mu}_2 - 2\hat{\lambda}_2(\hat{\mu}_1 + \hat{\mu}_2) - \hat{\lambda}_2\hat{\mu}_2)) \\ &- \cos(2\xi(2(\hat{\lambda}_1 + \hat{\lambda}_2)(\hat{\mu}_1 + \hat{\mu}_2) + (\hat{\lambda}_1 + \hat{\lambda}_2)\hat{\mu}_2 + \hat{\lambda}_2(\hat{\mu}_1 + \hat{\mu}_2) - \hat{\lambda}_2\hat{\mu}_2)) \\ &- \cos(2\xi(-(\hat{\lambda}_1 + \hat{\lambda}_2)(\hat{\mu}_1 + \hat{\mu}_2) + (\hat{\lambda}_1 + \hat{\lambda}_2)\hat{\mu}_2 + \hat{\lambda}_2(\hat{\mu}_1 + \hat{\mu}_2) + 2\hat{\lambda}_2\hat{\mu}_2)) \end{aligned} \right],$$

where $\xi = \pi/3(k+4)$, $\lambda = (\lambda_1, \lambda_2)$, $\mu = (\mu_1, \mu_2)$, and $\hat{\lambda}_i = \lambda_i + 1$, $\hat{\mu}_i = \mu_i + 1$ for $i = 1, 2$.

Letting $\hat{\mu}_1 = 3(k+4)x_1$, $\hat{\mu}_2 = -(k+4)x_2$, we obtain

$$S_{\lambda,\mu} = \frac{-2}{(k+4)\sqrt{3}} \left[\cos(2\pi((2\hat{\lambda}_1 + 3\hat{\lambda}_2)x_1 - (\hat{\lambda}_1 + 2\hat{\lambda}_2)x_2)) + \cos(2\pi((\hat{\lambda}_1 + 3\hat{\lambda}_2)x_1 - \hat{\lambda}_2x_2)) \right. \\ \left. + \cos(2\pi(\hat{\lambda}_1x_1 - (\hat{\lambda}_1 + \hat{\lambda}_2)x_2)) - \cos(2\pi((\hat{\lambda}_1 + 3\hat{\lambda}_2)x_1 - (\hat{\lambda}_1 + 2\hat{\lambda}_2)x_2)) \right. \\ \left. - \cos(2\pi((2\hat{\lambda}_1 + 3\hat{\lambda}_2)x_1 - (\hat{\lambda}_1 + \hat{\lambda}_2)x_2)) - \cos(2\pi(\hat{\lambda}_1x_1 + 2\hat{\lambda}_2x_2)) \right],$$

which is (up to a scalar factor) nothing but the S -function $S_{\lambda+\varrho}(x)$ (see [25, Section 2.3] for a discussion on orbit functions). Then we see that

$$\beta_{\lambda}^{(\mu)} = \frac{S_{\lambda,\mu}}{S_{0,\mu}} = \frac{S_{\lambda+\varrho}(x)}{S_{\varrho}(x)} = \chi_{\lambda}(t_{\nu}) \in \chi_{\lambda}(\mathbb{T}^2) = I_{\lambda}, \quad (35)$$

where $t_{\nu} = (e^{2\pi i x_1}, e^{2\pi i x_2})$, and hence the spectrum $\sigma(G_{\lambda})$ of G_{λ} is contained in I_{λ} . Note that here we are using the Dynkin labels whereas in Section 2 we used labels $(\mu_1, \mu_2) = (\lambda_1 + \lambda_2, \lambda_2)$.

Consider now the pair of nimrep graphs G_{λ} , G_{μ} , which have joint spectrum $\mathfrak{D}_{\lambda,\mu} \subset I_{\lambda} \times I_{\mu}$. The m, n^{th} cross moment $\varsigma_{m,n} = \int_{\mathfrak{D}_{\lambda,\mu}} x^m y^n d\tilde{\nu}(x, y)$, where $x = x_{\lambda}$, $y = x_{\mu}$, is given by $\langle G_{\lambda}^m G_{\mu}^n \Omega, \Omega \rangle$. Let $\beta_{\lambda}^{(\sigma)}$ be the eigenvalues of G_{λ} with corresponding eigenvectors $\psi^{(\sigma)}$, normalized so that each $\psi^{(\sigma)}$ has norm 1. As the nimreps are a family of commuting matrices they can be simultaneously diagonalised, and thus the eigenvectors of G_{λ} are the same for all λ . Then $G_{\lambda}^m G_{\mu}^n = \mathcal{U} \Lambda_{\lambda}^m \Lambda_{\mu}^n \mathcal{U}^*$, where Λ_{λ} is the diagonal matrix with the eigenvalues $\beta_{\lambda}^{(\sigma)}$ on the diagonal, and \mathcal{U} is the unitary matrix whose columns are given by the eigenvectors $\psi^{(\sigma)}$, so that

$$\varsigma_{m,n} = \langle \mathcal{U} \Lambda_{\lambda}^m \Lambda_{\mu}^n \mathcal{U}^* \Omega, \Omega \rangle = \langle \Lambda_{\lambda}^m \Lambda_{\mu}^n \mathcal{U}^* \Omega, \mathcal{U}^* \Omega \rangle = \sum_{\sigma} (\beta_{\lambda}^{(\sigma)})^m (\beta_{\mu}^{(\sigma)})^n |\psi_{*}^{(\sigma)}|^2, \quad (36)$$

where $\psi_{*}^{(\sigma)} = \mathcal{U}^* \Omega$ is the entry of the eigenvector $\psi^{(\sigma)}$ corresponding to the distinguished vertex $*$. Thus there is a D_{12} -invariant measure ε over \mathbb{T}^2 such that

$$\varsigma_{m,n} = \int_{\mathbb{T}^2} \chi_{\lambda}(\omega_1, \omega_2)^m \chi_{\mu}(\omega_1, \omega_2)^n d\varepsilon(\omega_1, \omega_2),$$

for all λ, μ .

Note from (35), (36) that the measure ε is a discrete measure which has weight $|\psi_{*}^{(\nu)}|^2$ at the points $g(t_{\nu}) \in \mathbb{T}^2$ for $g \in D_{12}$, $\nu \in \text{Exp}(G)$, and zero everywhere else. Thus the measure ε does not depend on the choice of λ, μ , so that the measure over \mathbb{T}^2 is the same for any pair (G_{λ}, G_{μ}) , even though the corresponding measures over $\mathfrak{D}_{\lambda,\mu} \subset \mathbb{R}^2$, and indeed the subsets $\mathfrak{D}_{\lambda,\mu}$ themselves, are different for each such pair.

We will now determine this D_{12} -invariant measure ε over \mathbb{T}^2 for all the known G_2 modular invariants, where we will focus in particular on the nimrep graphs for the fundamental generators ρ_j , $j = 1, 2$, which have quantum dimensions $[2][7][12]/[4][6]$, $[7][8][15]/[3][4][5]$ respectively, where $[m]$ denotes the quantum integer $[m] = (q^m - q^{-m})/(q - q^{-1})$ for $q = e^{i\pi/3(k+4)}$. The nimrep graphs G_{ρ_1} were found in [14], whilst G_{ρ_2} for the conformal embeddings at levels 3, 4 were found in [13]. The realisation of modular invariants

for G_2 by braided subfactors is parallel to the realisation of $SU(2)$ and $SU(3)$ modular invariants by α -induction for a suitable braided subfactors [34, 36, 44, 3, 4, 8, 9], [35, 36, 44, 3, 4, 8, 6, 7, 19, 20] respectively. The realisation of modular invariants for C_2 is also under way [25].

5.1 Graphs $\mathcal{A}_k(G_2)$, $k \leq \infty$

The graphs $\mathcal{A}_k^{\rho_j}(G_2)$, $j = 1, 2$, are associated with the trivial G_2 modular invariant at level k . They are illustrated in Figures 5, 6 respectively, where the set of vertices is now given by P_{++}^k . The set of edges is given by the edges between these vertices, except for certain self-loops at the cut-off which are indicated by dashed lines (in Figures 5, 6 the dashed lines indicate the edges to be removed when $k = 6$). The eigenvalues $\beta^{j,(\lambda)} := \beta_{\rho_j}^{(\lambda)}$ of $\mathcal{A}_k^{\rho_j}(G_2)$, $j = 1, 2$, are given by the ratio $S_{\rho_j, \lambda}/S_{0, \lambda}$ with corresponding eigenvectors $\psi_\mu^\lambda = S_{\lambda, \mu}$, where $\mu \in \text{Exp}(\mathcal{A}_k(G_2)) = P_{++}^k$. Then with $\mu = * = (0, 0)$, we obtain

$$\begin{aligned} \psi_*^\lambda = \frac{-2}{(k+4)\sqrt{3}} & \left[\cos(2\xi(5\hat{\lambda}_1 + 9\hat{\lambda}_2)) + \cos(2\xi(\hat{\lambda}_1 + 6\hat{\lambda}_2)) + \cos(2\xi(4\hat{\lambda}_1 + 3\hat{\lambda}_2)) \right. \\ & \left. - \cos(2\xi(4\hat{\lambda}_1 + 9\hat{\lambda}_2)) - \cos(2\xi(\hat{\lambda}_1 - 3\hat{\lambda}_2)) - \cos(2\xi(5\hat{\lambda}_1 + 6\hat{\lambda}_2)) \right] \end{aligned} \quad (37)$$

and hence we see that

$$\psi_*^\lambda = \frac{-1}{4\sqrt{3}(k+4)\pi^2} J\left((\hat{\lambda}_1 + 3\hat{\lambda}_2)/3(k+4), -\hat{\lambda}_1/3(k+4)\right), \quad (38)$$

where $J(\theta_1, \theta_2)$ is given by (28) and in (38) we have

$$\theta_1 = (\hat{\lambda}_1 + 3\hat{\lambda}_2)/3(k+4), \quad \theta_2 = -\hat{\lambda}_1/3(k+4), \quad (39)$$

so that $\hat{\lambda}_1 = -3(k+4)\theta_2$ and $\hat{\lambda}_2 = (k+4)(\theta_1 + \theta_2)$.

As a consequence of the identification (38) between the Perron-Frobenius eigenvector and the Jacobian we can obtain another expression for the Jacobian J . Recall that the Perron-Frobenius eigenvector for $\mathcal{A}_k(G_2)$ can also be written in the Kac-Weyl factorized form [32]:

$$\phi_\lambda^* = \frac{\sin(\hat{\lambda}_1\xi) \sin(3\hat{\lambda}_2\xi) \sin((\hat{\lambda}_1 + 3\hat{\lambda}_2)\xi) \sin((2\hat{\lambda}_1 + 3\hat{\lambda}_2)\xi) \sin((3\hat{\lambda}_1 + 3\hat{\lambda}_2)\xi) \sin((3\hat{\lambda}_1 + 6\hat{\lambda}_2)\xi)}{\sin(\xi) \sin(3\xi) \sin(4\xi) \sin(5\xi) \sin(6\xi) \sin(9\xi)}. \quad (40)$$

Now $\phi_*^* = 1$ whilst $\psi_*^* = -2[\cos(28\xi) + 2\cos(14\xi) - \cos(26\xi) - \cos(22\xi) - \cos(4\xi)]/(k+4)\sqrt{3} = 64\sin(\xi) \sin(3\xi) \sin(4\xi) \sin(5\xi) \sin(6\xi) \sin(9\xi)/(k+4)\sqrt{3}$. Thus we see that $(k+4)\sqrt{3}\psi_*^* = 64\sin(\xi) \sin(3\xi) \sin(4\xi) \sin(5\xi) \sin(6\xi) \sin(9\xi)\phi_*^*$. Then from (38) we have

$$\begin{aligned} J(\theta_1, \theta_2) &= -4(k+4)\sqrt{3}\pi^2 \psi_*^{(-3(k+4)(\theta_2-1), (k+4)(\theta_1+\theta_2-1))} \\ &= -256\pi^2 \sin(\xi) \sin(3\xi) \sin(4\xi) \sin(5\xi) \sin(6\xi) \sin(9\xi) \phi_{(-3(k+4)(\theta_2-1), (k+4)(\theta_1+\theta_2-1))}^* \\ &= 256\pi^2 \sin(\theta_1\pi) \sin(\theta_2\pi) \sin((\theta_1 + \theta_2)\pi) \sin((\theta_1 - \theta_2)\pi) \sin((2\theta_1 - \theta_2)\pi) \sin((\theta_1 - 2\theta_2)\pi), \end{aligned}$$

so that the Jacobian $J(\theta_1, \theta_2)$ can also be written as a product of sine functions.

The eigenvalues $\beta^{j,(\lambda)} = S_{\rho_j, \lambda} / S_{0, \lambda}$ are given by

$$\begin{aligned}\beta^{1,(\lambda)} &= 1 + 2 \cos(2\xi \hat{\lambda}_1) + 2 \cos(2\xi(\hat{\lambda}_1 + 3\hat{\lambda}_2)) + 2 \cos(2\xi(2\hat{\lambda}_1 + 3\hat{\lambda}_2)) = \chi_1(\omega_1, \omega_2), \\ \beta^{2,(\lambda)} &= 2 + 2 \cos(2\xi \hat{\lambda}_1) + 2 \cos(2\xi(\hat{\lambda}_1 + 3\hat{\lambda}_2)) + 2 \cos(2\xi(2\hat{\lambda}_1 + 3\hat{\lambda}_2)) \\ &\quad + 2 \cos(6\xi \hat{\lambda}_2) + 2 \cos(6\xi(\hat{\lambda}_1 + \hat{\lambda}_2)) + 2 \cos(6\xi(\hat{\lambda}_1 + 2\hat{\lambda}_2)) = \chi_2(\omega_1, \omega_2),\end{aligned}$$

where $\omega_j = \exp^{2\pi i \theta_j}$, $j = 1, 2$ are related to λ as in (39).

We now compute the spectral measure for $\mathcal{A}_k^{\rho_j}(G_2)$. Now summing over all $(\lambda_1, \lambda_2) \in \text{Exp}(\mathcal{A}_k(G_2))$ corresponds to summing over all $(\theta_1, \theta_2) \in \{((\hat{\lambda}_1 + 3\hat{\lambda}_2)/3(k+4), -\hat{\lambda}_1/3(k+4)) \mid \hat{\lambda}_1, \hat{\lambda}_2 \geq 1, \hat{\lambda}_1 + 2\hat{\lambda}_2 \leq k+3\}$, or equivalently, since such points satisfy $\theta_1 + \theta_2 \equiv 0 \pmod{3}$, to summing over all $(\theta_1, \theta_2) \in F'_k = \{(q_1/3(k+4), q_2/3(k+4)) \mid q_1, q_2 = 0, 1, \dots, 3k+11; q_1 + q_2 \equiv 0 \pmod{3}\}$ such that

$$\begin{aligned}\theta_2 &= -\hat{\lambda}_1/3(k+4) \leq -1/3(k+4), & \theta_1 + \theta_2 &= \hat{\lambda}_2/(k+4) \geq 1/(k+4) \\ 2\theta_1 - \theta_2 &= (\hat{\lambda}_1 + 2\hat{\lambda}_2)/(k+4) \leq (k+3)/(k+4) = 1 - 1/(k+4).\end{aligned}$$

Since θ_j and $\theta_j + n$ give the same points in \mathbb{T}^2 for $n \in \mathbb{Z}$, the last three conditions are equivalent to

$$\theta_2 \leq 1 - 1/3(k+4), \quad \theta_1 + \theta_2 \geq 1 + 1/(k+4), \quad 2\theta_1 - \theta_2 \leq -1/(k+4).$$

Denote by F_k the set of all $(\omega_1, \omega_2) \in \mathbb{T}^2$ such that $(\theta_1, \theta_2) \in F'_k$ satisfies these conditions. Then from (36) and (38) we obtain

$$\begin{aligned}\varsigma_{m,n} &= \frac{1}{48(k+4)^2\pi^4} \sum_{\lambda \in \text{Exp}} (\beta^{1,(\lambda)})^m (\beta^{2,(\lambda)})^n J((\lambda_1 + 3\lambda_2)/3(k+4), -\lambda_1/3(k+4))^2 \\ &= \frac{1}{48(k+4)^2\pi^4} \sum_{(\omega_1, \omega_2) \in F_k} (\chi_1(\omega_1, \omega_2))^m (\chi_2(\omega_1, \omega_2))^n J(\omega_1, \omega_2)^2\end{aligned} \quad (41)$$

If we let F be the limit of F_k as $k \rightarrow \infty$, then F is a fundamental domain of \mathbb{T}^2 under the action of the group D_{12} , illustrated in Figure 8. Since $J = 0$ along the boundary of F , which is mapped to the boundary of \mathfrak{D} under $\Psi : \mathbb{T}^2 \rightarrow \mathfrak{D}$, we can include points on the boundary of F in the summation in (41). Since J^2 is invariant under the action of D_{12} , we have

$$\varsigma_{m,n} = \frac{1}{12} \frac{1}{48(k+4)^2\pi^4} \sum_{(\omega_1, \omega_2) \in F_k^W} (\chi_1(\omega_1, \omega_2))^m (\chi_2(\omega_1, \omega_2))^n J(\omega_1, \omega_2)^2 \quad (42)$$

where

$$F_k^W = \{(e^{2\pi i q_1/3(k+4)}, e^{2\pi i q_2/3(k+4)}) \in \mathbb{T}^2 \mid q_1, q_2 = 0, 1, \dots, 3k+11; q_1 + q_2 \equiv 0 \pmod{3}\} \quad (43)$$

is the image of F_k under the action of the Weyl group $W = D_{12}$ and some additional points which lie on the boundaries of the fundamental domains (i.e. where $J = 0$). We illustrate the points (θ_1, θ_2) such that $(e^{2\pi i \theta_1}, e^{2\pi i \theta_2}) \in F_2^W$ in Figure 16. The points in the interior of the fundamental domain F , those enclosed by the dashed line, correspond to the vertices of the graph $\mathcal{A}_2(G_2)$.

Note that $F_k^W = D_{k+4}$ in the notation of [21, §7.1], and that $|F_k^W| = 3(k+4)^2$. Thus from (42), we obtain (c.f. [21, Theorem 4]):

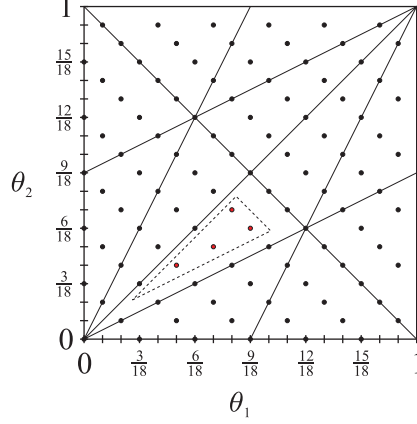


Figure 16: The points (θ_1, θ_2) such that $(e^{2\pi i \theta_1}, e^{2\pi i \theta_2}) \in F_2^W$.

Theorem 5.1. *The joint spectral measure of $\mathcal{A}_k^{\rho_j}(G_2)$, $j = 1, 2$, (over \mathbb{T}^2) is given by*

$$d\varepsilon(\omega_1, \omega_2) = \frac{1}{192\pi^4} J(\omega_1, \omega_2)^2 d^{(k+4)}(\omega_1, \omega_2), \quad (44)$$

where $d^{(k+4)}$ is the uniform measure over F_k^W .

In fact, the spectral measure over \mathbb{T}^2 for the nimrep graph G_λ for any $\lambda \in {}_N\mathcal{X}_N$ (where $G_{\rho_j} = \mathcal{A}_k^{\rho_j}(G_2)$) is given by the above measure.

We can now easily deduce the spectral measure (over \mathbb{T}^2) for $\mathcal{A}_\infty(G_2)$ claimed in Section 4.1. Letting $k \rightarrow \infty$, the measure $d^{(k+4)}(\omega_1, \omega_2)$ becomes the uniform Lebesgue measure $d\omega_1 d\omega_2$ on \mathbb{T}^2 . Thus:

Theorem 5.2. *The joint spectral measure of the infinite graph $\mathcal{A}_\infty(G_2)$ (over \mathbb{T}^2) is given by*

$$d\varepsilon(\omega_1, \omega_2) = \frac{1}{192\pi^4} J(\omega_1, \omega_2)^2 d\omega_1 d\omega_2, \quad (45)$$

where $d\omega$ is the uniform Lebesgue measure over \mathbb{T} .

Then the spectral measure for $\mathcal{A}_k^{\rho_j}(G_2)$ over \mathfrak{D} or I_j , $j = 1, 2$, has the same weights as the spectral measure for the infinite graph $\mathcal{A}_\infty^{\rho_j}(G_2)$ given in Section 4.2, but the measure here is a discrete measure.

5.2 Exceptional Graph $\mathcal{E}_3(G_2)$: $(G_2)_3 \rightarrow (E_6)_1$

The graph $\mathcal{E}_3(G_2) := \mathcal{E}_3^{\rho_1}(G_2) = \mathcal{E}_3^{\rho_2}(G_2)$, illustrated in Figure 17, is the nimrep graph associated to the conformal embedding $(G_2)_3 \rightarrow (E_6)_1$, and is one of two nimrep graphs associated to the modular invariant

$$Z_{\mathcal{E}_3} = |\chi_{(0,0)} + \chi_{(1,1)}|^2 + 2|\chi_{(2,0)}|^2$$

which is at level 3 and has exponents $\text{Exp}(\mathcal{E}_3(G_2)) = \{(0,0), (1,1), \text{ and } (2,0) \text{ twice}\}$. The other nimrep graph associated to this modular invariant is $\mathcal{E}_3^M(G_2)$ considered in the next section.

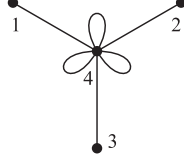


Figure 17: Exceptional Graph $\mathcal{E}_3(G_2)$

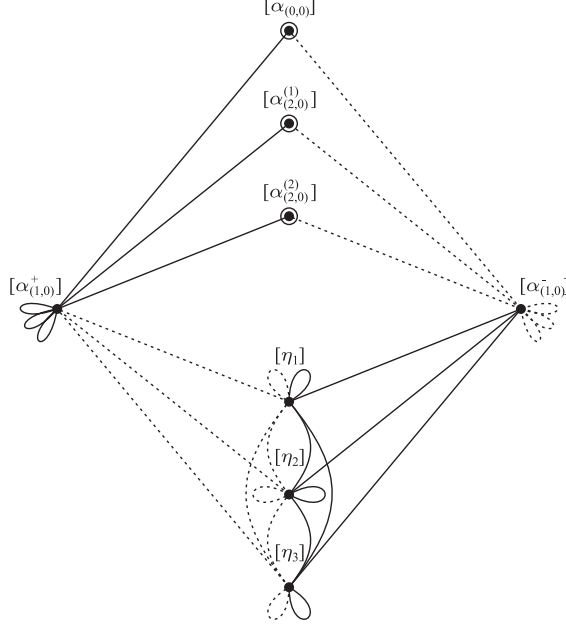


Figure 18: $\mathcal{E}_3(G_2)$: Multiplication by $[\alpha_{(1,0)}^+]$ (solid lines) and $[\alpha_{(1,0)}^-]$ (dashed lines)

Following [4, §6] we can compute the principal graph and dual principal graph of the inclusion $(G_2)_3 \rightarrow (E_6)_1$. The chiral induced sector bases ${}_M\mathcal{X}_M^\pm \subset \text{Sect}(M)$ and full induced sector basis ${}_M\mathcal{X}_M \subset \text{Sect}(M)$, the sector bases given by all irreducible subsectors of $[\alpha_\lambda^\pm]$ and $[\alpha_\lambda^+ \circ \alpha_{\lambda'}^-]$ respectively, for $\lambda, \lambda' \in {}_N\mathcal{X}_N$, are given by

$$\begin{aligned} {}_M\mathcal{X}_M^\pm &= \{[\alpha_{(0,0)}], [\alpha_{(1,0)}^\pm], [\alpha_{(2,0)}^{(1)}], [\alpha_{(2,0)}^{(2)}]\}, \\ {}_M\mathcal{X}_M &= \{[\alpha_{(0,0)}], [\alpha_{(1,0)}^+], [\alpha_{(1,0)}^-], [\alpha_{(2,0)}^{(1)}], [\alpha_{(2,0)}^{(2)}], [\eta_1], [\eta_2], [\eta_3]\}, \end{aligned}$$

where $[\alpha_{(2,0)}^\pm] = [\alpha_{(1,0)}^\pm] \oplus [\alpha_{(2,0)}^{(1)}] \oplus [\alpha_{(2,0)}^{(2)}]$, $[\alpha_{(1,0)}^+ \circ \alpha_{(1,0)}^-] = [\eta_1] \oplus [\eta_2] \oplus [\eta_3]$, and $\alpha_{(i,j)} \equiv \alpha_{\lambda_{(i,j)}}$. The fusion graphs of $[\alpha_{(1,0)}^+]$ (solid lines) and $[\alpha_{(1,0)}^-]$ (dashed lines) are given in Figure 18, see also [13, Figure 17(a)]. The marked vertices corresponding to sectors in ${}_M\mathcal{X}_M^0 = {}_M\mathcal{X}_M^+ \cap {}_M\mathcal{X}_M^-$ have been circled. Note that multiplication by $[\alpha_{(1,0)}^+]$ (or $[\alpha_{(1,0)}^-]$) does not give two copies of the nimrep graph $\mathcal{E}_3(G_2)$ as one might expect, but rather one copy each of $\mathcal{E}_3(G_2)$ and $\mathcal{E}_3^M(G_2)$. This is similar to the situation for the $SU(3)$ conformal embedding $SU(3)_9 \rightarrow (E_6)_1$ [15, §5.2].

Let $\iota : N \hookrightarrow M$ denote the injection map $\iota(n) = n \in M$, $n \in N$ and $\bar{\iota}$ its conjugate. The dual canonical endomorphism $\theta = \bar{\iota} \circ \iota$ for the conformal embedding can be read from

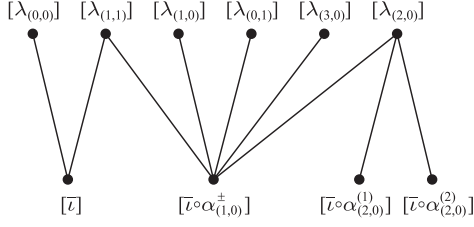


Figure 19: $\mathcal{E}_3(G_2)$: Principal graph of $(G_2)_3 \rightarrow (E_6)_1$

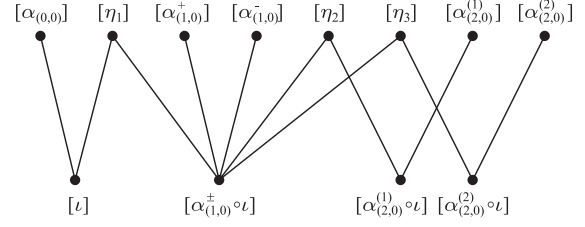


Figure 20: $\mathcal{E}_3(G_2)$: Dual principal graph of $(G_2)_3 \rightarrow (E_6)_1$



Figure 21: $\mathcal{E}_3(G_2)$: Principal graph of $\alpha_{(1,0)}^\pm(M) \subset M$

the vacuum block of the modular invariant: $[\theta] = [\lambda_{(0,0)}] \oplus [\lambda_{(1,1)}]$. By [4, Corollary 3.19] and the fact that $\langle \gamma, \gamma \rangle_M = \langle \theta, \theta \rangle_N = 2$, the canonical endomorphism $\gamma = \iota \circ \bar{\iota}$ is given by

$$[\gamma] = [\alpha_{(0,0)}] \oplus [\eta_1]. \quad (46)$$

Then by [4, Theorem 4.2], the principal graph of the inclusion $(G_2)_3 \rightarrow (E_6)_1$ of index $\frac{1}{2}(7 + \sqrt{21}) \approx 5.79$ is given by the connected component of $[\lambda_{(0,0)}] \in {}_N\mathcal{X}_N$ of the induction-restriction graph, and the dual principal graph is given by the connected component of $[\alpha_{(0,0)}] \in {}_M\mathcal{X}_M$ of the γ -multiplication graph. The principal graph and dual principal graph are illustrated in Figures 19 and 20 respectively. These principal graphs are sometimes referred to as “Haagerup with legs” [31, §4.2.4]. The principal graph in Figure 19 appears as the intertwiner for the quantum subgroup $\mathcal{E}_3(G_2)$ in [13, §4.4].

One can also construct a subfactor $\alpha_{(1,0)}^\pm(M) \subset M$ with index $(\frac{1}{2}(3 + \sqrt{21}))^2 = \frac{3}{2}(5 + \sqrt{21}) \approx 14.37$, where M is a type III factor. This subfactor has already appeared in [29, 45] (see also the Appendix in [11], [31] and [17]). The chiral systems ${}_M\mathcal{X}_M^\pm$ are near group C^* -category of type $G + 3$, where $G = \mathbb{Z}_3$, generated by a self-conjugate irreducible endomorphism ρ of M and an outer action α of G on M , such that $[\alpha_i][\rho] = [\rho] = [\rho][\alpha_i]$ and $[\rho^2] = \bigoplus_{i=1}^3 [\alpha_i] \oplus 3[\rho]$, for $i \in \mathbb{Z}_3$. Here $\alpha_{(1,0)}^\pm = \rho$, $\alpha_{(0,0)} = \alpha_0$ and $\alpha_{(2,0)}^{(j)} = \alpha_j$. The index d_ρ^2 of $\rho(M) \subset M$ is thus $d_\rho^2 = 3d_\rho + 3$, where d_σ is the statistical dimension of σ . Its principal graph is illustrated in Figure 21 and is the bipartite unfolded version of the graph $\mathcal{E}_3(G_2)$. The dual principal graph is isomorphic to the principal graph as abstract graphs [44, Corollary 3.7].

We now determine the joint spectral measure of $\mathcal{E}_3^{\rho_1}(G_2)$, $\mathcal{E}_3^{\rho_2}(G_2)$. With θ_1, θ_2 as in (39) for $\lambda = (\lambda_1, \lambda_2) \in \text{Exp}(\mathcal{E}_3(G_2))$, we have the following values:

$\lambda \in \text{Exp}$	$(\theta_1, \theta_2) \in [0, 1]^2$	$ \psi_*^\lambda ^2$	$\frac{1}{8\pi^2} J(\theta_1, \theta_2) $
$(0, 0)$	$(\frac{4}{21}, \frac{20}{21})$	$\frac{7-\sqrt{21}}{42}$	$\frac{7-\sqrt{21}}{4}$
$(1, 1)$	$(\frac{8}{21}, \frac{19}{21})$	$\frac{7+\sqrt{21}}{42}$	$\frac{7+\sqrt{21}}{4}$
$(2, 0)$	$(\frac{2}{7}, \frac{6}{7})$	$\frac{1}{2}$	$\frac{7}{2}$

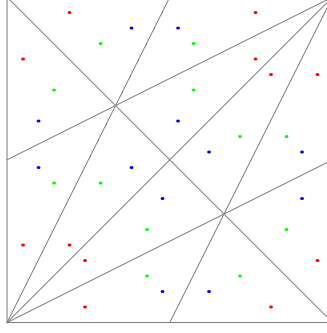


Figure 22: The orbit of the points (θ_1, θ_2) for $\lambda \in \text{Exp}(\mathcal{E}_3(G_2))$.

where the eigenvectors ψ^λ have been normalized so that $\|\psi^\lambda\| = 1$, and for the exponent $(2, 0)$ which has multiplicity two, the value listed in the table for $|\psi_*^{(2,0)}|^2$ is $|\psi_*^{(2,0)_1}|^2 + |\psi_*^{(2,0)_2}|^2$. Note that

$$|\psi_*^\lambda|^2 = \frac{2}{21} \left(\frac{1}{8\pi^2} |J| \right) + \zeta_\lambda \quad (47)$$

where $\zeta_\lambda = 0$ for $\lambda \in \{(0, 0), (1, 1)\}$ and $\zeta_{(2,0)} = 1/6$.

The orbit under D_{12} of the points $(\theta_1, \theta_2) \in \left\{ \left(\frac{4}{21}, \frac{20}{21} \right), \left(\frac{8}{21}, \frac{19}{21} \right), \left(\frac{2}{7}, \frac{6}{7} \right) \right\}$ are illustrated in Figure 22. These points give the measure $d^{(21/4, 1/21)}$, whose support has cardinality 36. Note that when taking the orbit under D_{12} , the associated weight in (47) is now counted 12 times, thus we must divide (47) by 12. Thus the measure for $\mathcal{E}_3(G_2)$ is

$$d\varepsilon = 36 \frac{1}{12} \frac{2}{21} \frac{1}{8\pi^2} |J| d^{(21/4, 1/21)} + \frac{\zeta_{(2,0)}}{12} \sum_{g \in D_{12}} \delta_{g(e^{4\pi i/7}, e^{6\pi i/7})},$$

where δ_x is the Dirac measure at the point x . Then we have obtained the following result:

Theorem 5.3. *The joint spectral measure of $\mathcal{E}_3^{\rho_1}(G_2)$, $\mathcal{E}_3^{\rho_2}(G_2)$ (over \mathbb{T}^2) is*

$$d\varepsilon = \frac{1}{28\pi^2} |J| d^{(21/4, 1/21)} + \frac{1}{72} \sum_{g \in D_{12}} \delta_{g(e^{4\pi i/7}, e^{6\pi i/7})}, \quad (48)$$

where $d^{(n,k)}$ is as in Definition 2.1 and δ_x is the Dirac measure at the point x .

5.3 Exceptional Graph $\mathcal{E}_3^M(G_2)$: $(G_2)_3 \rightarrow (E_6)_1 \rtimes \mathbb{Z}_3$

The graph $\mathcal{E}_3^M(G_2) := \mathcal{E}_3^{M, \rho_1}(G_2) = \mathcal{E}_3^{M, \rho_2}(G_2)$, illustrated in Figure 23, is the nimrep graph for the type II inclusion $(G_2)_3 \rightarrow (E_6)_1 \rtimes \mathbb{Z}_3$ with index $\frac{3}{2}(7 + \sqrt{21}) \approx 17.37$, where $\tau = \alpha_{(2,0)}^{(1)}$ is a non-trivial simple current of order 3 in the ambichiral system ${}_M\mathcal{X}_M^0$, see Figure 18. For such an orbifold inclusion to exist, one needs an automorphism τ_0 such that $[\tau_0] = [\tau]$ and $\tau_0^3 = \text{id}$ [3, §3], which exists precisely when the statistics phase ω_τ of τ satisfies $\omega_\tau^3 = 1$ [37, Lemma 4.4]. By [5, Lemma 6.1], if $[\tau]$ is a subsector of $[\alpha_\lambda^+]$ and $[\alpha_\mu^-]$ for some $\lambda, \mu \in {}_N\mathcal{X}_N$, then $\omega_\tau = \omega_\lambda = \omega_\mu$, and hence it is sufficient to check that

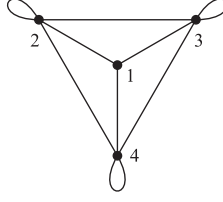


Figure 23: Exceptional Graph $\mathcal{E}_3^M(G_2)$

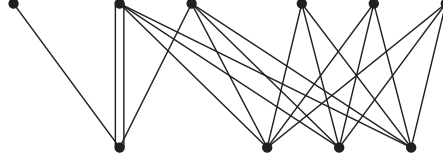


Figure 24: $\mathcal{E}_3^M(G_2)$: Principal graph of $(G_2)_3 \rightarrow (E_6)_1 \rtimes \mathbb{Z}_3$

ω_λ and ω_μ satisfy $\omega^3 = 1$. From Section 5.2, $[\tau] (= [\alpha_{(2,0)}^{(1)}])$ is a subsector of $[\alpha_{(2,0)}^\pm]$. Now $\omega_{(2,0)} = e^{4\pi i/3}$ [13, §4.4], which satisfies $\omega_{(2,0)}^3 = 1$, as required.

The principal graph for this inclusion is illustrated in Figure 24. This will be discussed in a future publication using a generalised Goodman-de la Harpe-Jones construction analogous to that for the D_{odd} and E_7 modular invariants for $SU(2)$ [9, §5.2, 5.3] and the type II inclusions for $SU(3)$ [20, §5]. It is not clear what the dual principal graph is in this case.

The associated modular invariant is again $Z_{\mathcal{E}_3}$ and the graph $\mathcal{E}_3^M(G_2)$ is isospectral to $\mathcal{E}_3(G_2)$. In fact, $\mathcal{E}_3^M(G_2)$ is obtained from $\mathcal{E}_3(G_2)$ by a \mathbb{Z}_3 -orbifold procedure. Then with θ_1, θ_2 as in (39) for $\lambda = (\lambda_1, \lambda_2) \in \text{Exp}(\mathcal{E}_3^M(G_2)) = \text{Exp}(\mathcal{E}_3(G_2))$, we have:

$\lambda \in \text{Exp}$	$(\theta_1, \theta_2) \in [0, 1]^2$	$ \psi_*^\lambda ^2$	$\frac{1}{64\pi^4} J(\theta_1, \theta_2)^2$
$(0, 0)$	$(\frac{4}{21}, \frac{20}{21})$	$\frac{7-\sqrt{21}}{14}$	$\frac{7(5-\sqrt{21})}{8}$
$(1, 1)$	$(\frac{8}{21}, \frac{19}{21})$	$\frac{7+\sqrt{21}}{14}$	$\frac{7(5+\sqrt{21})}{8}$
$(2, 0)$	$(\frac{2}{7}, \frac{6}{7})$	0	$\frac{49}{4}$

where the eigenvectors ψ^λ have been normalized so that $\|\psi^\lambda\| = 1$. In this case $\zeta_{(2,0)} = -1$ in (47). Thus we have the following result:

Theorem 5.4. *The joint spectral measure of $\mathcal{E}_3^{M,\rho_1}(G_2)$, $\mathcal{E}_3^{M,\rho_2}(G_2)$ (over \mathbb{T}^2) is*

$$d\varepsilon = \frac{3}{28\pi^2} |J| d^{(21/4, 1/21)} - \frac{1}{12} \sum_{g \in D_{12}} \delta_{g(e^{4\pi i/7}, e^{6\pi i/7})}, \quad (49)$$

where $d^{(n,k)}$ are as in Definition 2.1 and δ_x is the Dirac measure at the point x .

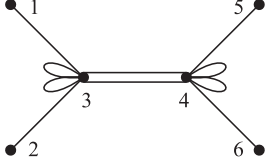


Figure 25: Graph $\mathcal{E}_4^{\rho_1}(G_2)$

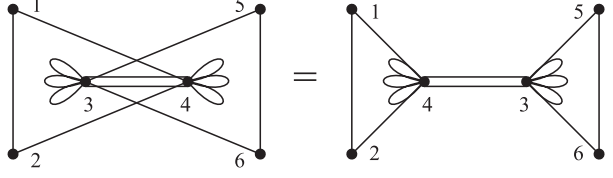


Figure 26: Graph $\mathcal{E}_4^{\rho_2}(G_2)$

5.4 Exceptional Graph $\mathcal{E}_4(G_2)$: $(G_2)_4 \rightarrow (D_7)_1$

The graphs $\mathcal{E}_4^{\rho_j}(G_2)$, illustrated in Figures 25 and 26, are the nimrep graphs associated with the conformal embedding $(G_2)_4 \rightarrow (D_7)_1 = (\text{Spin}(14))_1$ and are one of two families of graphs associated to the modular invariant

$$Z_{\mathcal{E}_4} = |\chi_{(0,0)} + \chi_{(3,0)}|^2 + |\chi_{(0,1)} + \chi_{(4,0)}|^2 + 2|\chi_{(1,1)}|^2$$

at level 4 with exponents $\text{Exp}(\mathcal{E}_4(G_2)) = \{(0,0), (3,0), (0,1), (4,0) \text{ and } (1,1) \text{ twice}\}$.

As in Section 5.2, we can compute the principal graph and dual principal graph of the inclusion $(G_2)_4 \rightarrow (D_7)_1$. The chiral induced sector bases ${}_M\mathcal{X}_M^\pm$ and full induced sector basis ${}_M\mathcal{X}_M$ are given by

$$\begin{aligned} {}_M\mathcal{X}_M^\pm &= \{[\alpha_{(0,0)}], [\alpha_{(1,0)}^\pm], [\alpha_{(0,2)}^\pm], [\alpha_{(0,1)}^{(1)}], [\alpha_{(1,1)}^{(1)}], [\alpha_{(1,1)}^{(2)}]\}, \\ {}_M\mathcal{X}_M &= \{[\alpha_{(0,0)}], [\alpha_{(1,0)}^+], [\alpha_{(1,0)}^-], [\alpha_{(0,2)}^+], [\alpha_{(0,2)}^-], [\alpha_{(0,1)}^{(1)}], [\alpha_{(1,1)}^{(1)}], [\alpha_{(1,1)}^{(2)}], [\eta_1], [\eta_2], [\zeta_1], [\zeta_2]\}, \end{aligned}$$

where $[\alpha_{(0,1)}^\pm] = [\alpha_{(0,2)}^\pm] \oplus [\alpha_{(0,1)}^{(1)}]$, $[\alpha_{(1,1)}^\pm] = [\alpha_{(1,0)}^\pm] \oplus [\alpha_{(0,2)}^\pm] \oplus [\alpha_{(1,1)}^{(1)}] \oplus [\alpha_{(1,1)}^{(2)}]$, $[\alpha_{(1,0)}^+ \circ \alpha_{(1,0)}^-] = [\eta_1] \oplus [\eta_2]$ and $[\alpha_{(1,0)}^+ \circ \alpha_{(0,2)}^-] = [\zeta_1] \oplus [\zeta_2]$. The fusion graphs of $[\alpha_{(1,0)}^+]$ (solid lines) and $[\alpha_{(1,0)}^-]$ (dashed lines) are given in Figure 27, where we have circled the marked vertices, and we note again that multiplication by $[\alpha_{(1,0)}^+]$ (or $[\alpha_{(1,0)}^-]$) gives one copy each of $\mathcal{E}_4(G_2)$ and $\mathcal{E}_4^M(G_2)$. The ambichiral part ${}_M\mathcal{X}_M^0$ obeys \mathbb{Z}_4 fusion rules, corresponding to D_7 at level 1.

We find

$$[\gamma] = [\alpha_{(0,0)}] \oplus [\eta_1], \quad (50)$$

and the principal graph and dual principal graph of the inclusion $(G_2)_4 \rightarrow (D_7)_1$ of index $6 + 2\sqrt{6} \approx 10.90$ are illustrated in Figures 28 and 29 respectively.

Again, we can construct a subfactor $\alpha_{(1,0)}^\pm(M) \subset M$ where M is a type III factor. Here the chiral systems ${}_M\mathcal{X}_M^\pm$ give quadratic extensions of a group category. Such fusion categories are discussed in [17, §1]. In our case, G is \mathbb{Z}_4 with subgroup $N = \mathbb{Z}_2$, $\rho = \alpha_{(1,0)}^\pm$ and $g_\rho = \text{id}$ since ρ is self-conjugate. The fusion rules are

$$[\alpha][\rho] = [\rho][\alpha] = [\rho\alpha] \neq [\rho], \quad [\alpha^2][\rho] = [\rho] = [\rho][\alpha^2], \quad (51)$$

$$[\rho]^2 = 2[\rho] \oplus 2[\rho\alpha] \oplus [\text{id}] \oplus [\alpha^2], \quad (52)$$

where $[\alpha]$ satisfies \mathbb{Z}_4 fusion rules, $[\text{id}] = [\alpha_{(0,0)}]$, $[\alpha] = [\alpha_{(1,1)}^{(1)}]$, $[\alpha^2] = [\alpha_{(0,1)}^{(1)}]$, $[\alpha^3] = [\alpha_{(1,1)}^{(2)}]$ and $[\rho\alpha] = [\alpha_{(0,2)}^\pm]$. Since $d_\alpha = 1$, the index d_ρ^2 of $\rho(M) \subset M$ satisfies $d_\rho^2 = 4d_\rho + 2$, thus $d_\rho^2 = (2 + \sqrt{6})^2 = 10 + 4\sqrt{6} \approx 19.80$. Its principal graph is illustrated in Figure 30 and

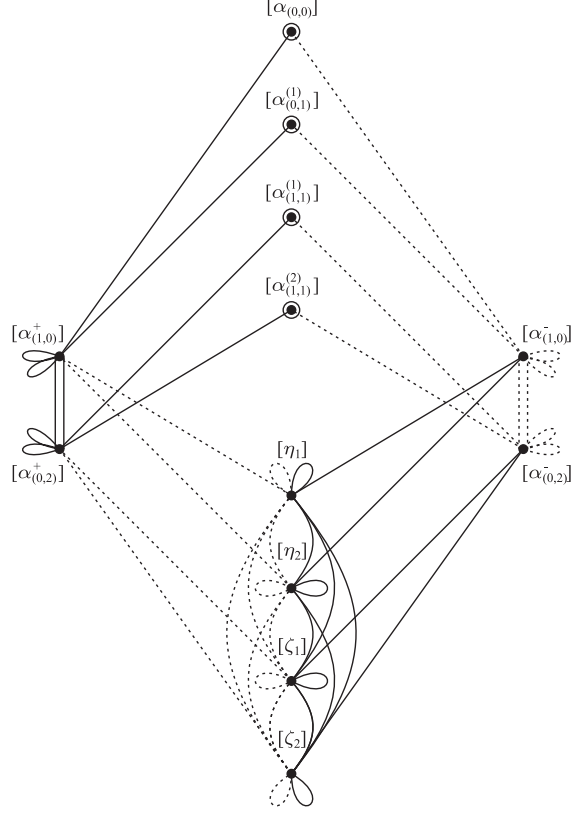


Figure 27: $\mathcal{E}_4(G_2)$: Multiplication by $[\alpha_{(1,0)}^+]$ (solid lines) and $[\alpha_{(1,0)}^-]$ (dashed lines)

is the bipartite unfolded version of the graph $\mathcal{E}_4^{\rho_1}(G_2)$. The dual principal graph is again isomorphic to the principal graph as abstract graphs.

For the fusion category above obtained from the conformal inclusion $(G_2)_4 \rightarrow (D_7)_1$, $\alpha_{(1,1)}^{(j)}$ is a non-trivial simple current of order 4 in ${}_M\mathcal{X}_M^0$, $j = 1, 2$. However, $[\alpha_{(1,1)}^{(j)}]$ is a subsector of $[\alpha_{(1,1)}^\pm]$, for which $\omega_{(1,1)} = e^{7\pi i/4}$ [13], thus $\omega_{(1,1)}^4 = e^{7\pi i} = -1$, and hence the orbifold inclusion $(G_2)_4 \rightarrow (D_7)_1 \rtimes_{\tau'} \mathbb{Z}_4$ does not exist (c.f. Section 5.3). On the other hand, the conformal dimension of the simple current $\alpha_{(0,1)}^\pm$ of order 2 is $1/2 \pmod{\mathbb{Z}}$. Thus one can choose an automorphism β on M such that $[\beta] = [\alpha^2] (= [\alpha_{(0,1)}^\pm])$ and $\beta^2 = \text{id}$. Thus there is an intermediate subfactor $\rho(M) \subset \rho(M) \rtimes \mathbb{Z}_2$ of index 2. The other intermediate subfactor $\rho(M) \rtimes \mathbb{Z}_2 \subset M$ would have index $5 + 2\sqrt{6}$. Writing

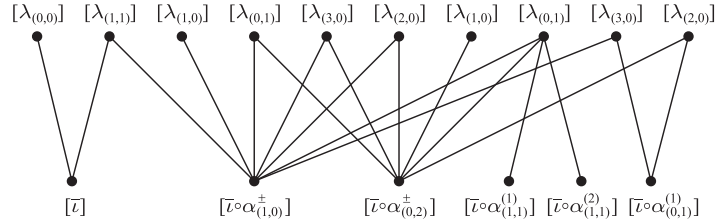


Figure 28: $\mathcal{E}_4(G_2)$: Principal graph of $(G_2)_4 \rightarrow (D_7)_1$

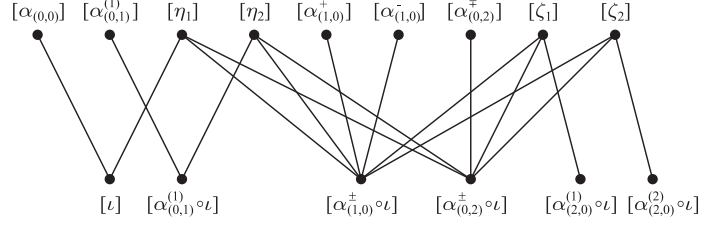


Figure 29: $\mathcal{E}_4(G_2)$: Dual principal graph of $(G_2)_4 \rightarrow (D_7)_1$

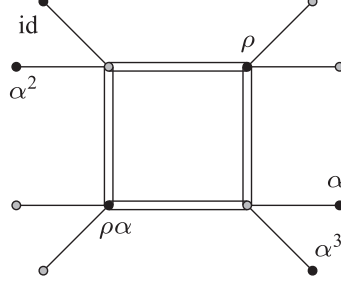


Figure 30: $\mathcal{E}_4(G_2)$: Principal graph of $\alpha_{(1,0)}^\pm(M) \subset M$

the inclusions as $\iota : \rho(M) \rightarrow \rho(M) \rtimes \mathbb{Z}_2$ and $j : \rho(M) \rtimes \mathbb{Z}_2 \rightarrow M$, as M - M sectors the canonical endomorphism $j\bar{j}$ is a subsector of the canonical endomorphism $j\iota\bar{j} = \rho^2$. Hence $[j\bar{j}]$ is a subsector of $2[\rho] \oplus 2[\rho\alpha] \oplus [\text{id}] \oplus [\beta]$ which contains $[\text{id}]$. By considering the statistical dimensions, we see that $[j\bar{j}] = [\text{id}] \oplus S$ for $S \in \{2[\rho], 2[\rho\alpha], [\rho] \oplus [\rho\alpha]\}$. The first two possibilities are not consistent with the fusion rules (51)-(52), so we obtain $[j\bar{j}] = [\text{id}] \oplus [\rho] \oplus [\rho\alpha]$, and the principal graph of $\rho(M) \rtimes \mathbb{Z}_2 \subset M$ is as in Figure 31.

We now determine the joint spectral measure of $\mathcal{E}_4^{\rho_1}(G_2)$, $\mathcal{E}_4^{\rho_2}(G_2)$. With θ_1, θ_2 as in (39) for $\lambda = (\lambda_1, \lambda_2) \in \text{Exp}(\mathcal{E}_4(G_2))$, we have:

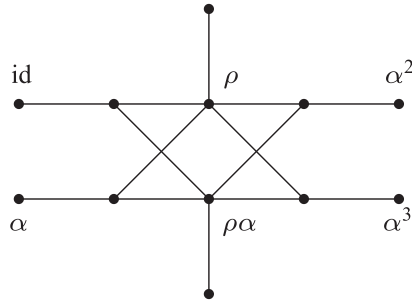


Figure 31: $\mathcal{E}_4(G_2)$: Principal graph of $\rho(M) \rtimes \mathbb{Z}_2 \subset M$

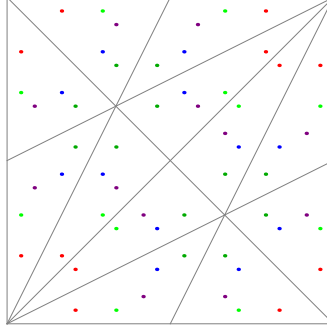


Figure 32: The orbit of the points (θ_1, θ_2) for $\lambda \in \text{Exp}(\mathcal{E}_4(G_2))$.

$\lambda \in \text{Exp}$	$(\theta_1, \theta_2) \in [0, 1]^2$	$ \psi_*^\lambda ^2$	$\frac{1}{8\pi^2} J(\theta_1, \theta_2) $
$(0, 0)$	$(\frac{1}{6}, \frac{23}{24})$	$\frac{3-\sqrt{6}}{24}$	$\frac{3-\sqrt{6}}{\sqrt{3}}$
$(3, 0)$	$(\frac{7}{24}, \frac{5}{6})$	$\frac{3+\sqrt{6}}{24}$	$\frac{3+\sqrt{6}}{\sqrt{3}}$
$(0, 1)$	$(\frac{7}{24}, \frac{23}{24})$	$\frac{1}{8}$	$\sqrt{3}$
$(4, 0)$	$(\frac{1}{3}, \frac{19}{24})$	$\frac{1}{8}$	$\sqrt{3}$
$(1, 1)$	$(\frac{1}{3}, \frac{11}{12})$	$0, \frac{1}{2}$	$2\sqrt{3}$

where again the eigenvectors ψ^λ have been normalized so that $\|\psi^\lambda\| = 1$. For the repeated exponent $(1, 1)$, one of the eigenvectors has $|\psi_*^{(1,1)1}|^2 = 0$ and the other has $|\psi_*^{(1,1)2}|^2 = 1/2$, thus their sum $|\psi_*^{(1,1)1}|^2 + |\psi_*^{(1,1)2}|^2 = 1/2$. Note that $24|\psi_*^\lambda|^2 = \sqrt{3}|J|/8\pi^2$ for $\lambda \in \{(0, 0), (3, 0)\}$, $3|\psi_*^\lambda|^2 = 2J^2/64\pi^4$ for $\lambda \in \{(0, 1), (4, 0)\}$ and $24(|\psi_*^{(1,1)1}|^2 + |\psi_*^{(1,1)2}|^2) = J^2/64\pi^4$.

The orbit under D_{12} of $(\theta_1, \theta_2) \in \{(\frac{1}{6}, \frac{23}{24}), (\frac{7}{24}, \frac{5}{6}), (\frac{7}{24}, \frac{23}{24}), (\frac{7}{24}, \frac{23}{24}), (\frac{1}{3}, \frac{11}{12})\}$ are illustrated in Figure 32. Let $\Upsilon_\lambda := \sum_{g \in D_{12}} (\beta^{(g(\lambda))})^m (\beta^{(g(\lambda))})^n |\psi_*^{g(\lambda)}|^2$. The orbits of the points $(1/6, 23/24)$ and $(7/24, 5/6)$ give the measure $d^{(6,1/24)}$, whose support has cardinality 36, but we have to remove the additional points $\{g(e^{\pi i/4}, e^{\pi i}) | g \in D_{12}\}$ which are in the support of $d^{(6,1/24)}$. For these additional points we have $|J| = 16\sqrt{2}\pi^2$. Thus $\Upsilon_{(0,0)} + \Upsilon_{(3,0)} = \frac{36}{12} \frac{\sqrt{3}}{24} \frac{1}{8\pi^2} |J| d^{(6,1/24)} - \frac{\sqrt{6}}{144} \sum_{g \in D_{12}} \delta_{g(e^{\pi i/4}, -1)}$. Now $\Upsilon_{(4,0)} = J^2/64\pi^4 d^{((6))}$ since $J(\theta_1, \theta_2) = 0$ for the additional points $(\theta_1, \theta_2) \in \text{Supp}(d^{((6))}) \setminus \{g(1/6, 19/24) | g \in D_{12}\} = \{g(1/6, 1/6) | g \in D_{12}\}$. We also have $\Upsilon_{(0,1)} = J^2/64\pi^4 d^{((8/3))}$ since again $J(\theta_1, \theta_2) = 0$ for the additional points in $\text{Supp}(d^{((8/3))})$, and similarly $\Upsilon_{(1,1)} = J^2/1024\pi^4 d^{((4))}$.

Thus we have the following result:

Theorem 5.5. *The joint spectral measure of $\mathcal{E}_4^{\rho_1}(G_2)$, $\mathcal{E}_4^{\rho_2}(G_2)$ (over \mathbb{T}^2) is*

$$\begin{aligned}
d\varepsilon = & \frac{\sqrt{3}}{64\pi^2} |J| d^{(6,1/24)} + \frac{1}{1024\pi^4} J^2 d^{((4))} + \frac{1}{64\pi^4} J^2 d^{((6))} + \frac{1}{64\pi^4} J^2 d^{((8/3))} \\
& - \frac{\sqrt{6}}{144} \sum_{g \in D_{12}} \delta_{g(e^{\pi i/4}, -i)},
\end{aligned} \tag{53}$$

where $d^{((n))}$, $d^{(n,k)}$ are as in Definition 2.1 and δ_x is the Dirac measure at the point x .

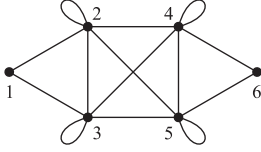


Figure 33: Graph $\mathcal{E}_4^{M, \rho_1}(G_2)$

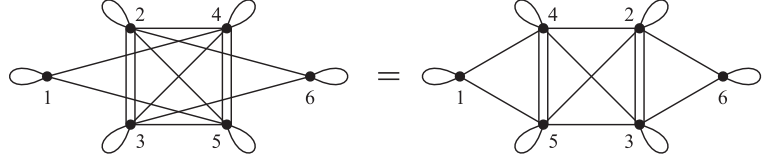


Figure 34: Graph $\mathcal{E}_4^{M, \rho_2}(G_2)$

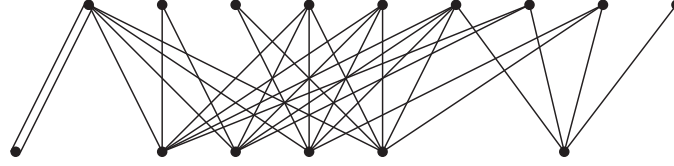


Figure 35: $\mathcal{E}_4^M(G_2)$: Principal graph of $(G_2)_4 \rightarrow (D_7)_1 \rtimes \mathbb{Z}_2$

5.5 Exceptional Graph $\mathcal{E}_4^M(G_2)$: $(G_2)_4 \rightarrow (D_7)_1 \rtimes \mathbb{Z}_2$

The graphs $\mathcal{E}_4^{M, \rho_j}(G_2)$, illustrated in Figures 33 and 34 are the nimrep graphs for the type II inclusion $(G_2)_4 \rightarrow (D_7)_1 \rtimes_{\tau} \mathbb{Z}_2$ with index $12 + 4\sqrt{6} \approx 21.80$, where $\tau = \alpha_{(0,1)}^{(1)}$ is a non-trivial simple current of order 2 in the ambichiral system ${}_M\mathcal{X}_M^0$, see Section 5.4. The principal graph for this inclusion is illustrated in Figure 35, which will be discussed in a future publication using a generalised Goodman-de la Harpe-Jones construction (c.f. the comments in Section 5.3). Again, it is not clear what the dual principal graph is in this case.

The associated modular invariant is again $Z_{\mathcal{E}_4}$ and the graphs are isospectral to $\mathcal{E}_4^{\rho_j}(G_2)$, with $\mathcal{E}_4^{M, \rho_j}(G_2)$ obtained from $\mathcal{E}_4^{\rho_j}(G_2)$ by a \mathbb{Z}_2 -orbifold procedure. However, the eigenvectors ψ^{λ} are not identical to those for $\mathcal{E}_4^{\rho_j}(G_2)$. With θ_1, θ_2 as in (39) for $\lambda = (\lambda_1, \lambda_2) \in \text{Exp}(\mathcal{E}_4^M(G_2)) = \text{Exp}(\mathcal{E}_4(G_2))$, we have:

$\lambda \in \text{Exp}$	$(\theta_1, \theta_2) \in [0, 1]^2$	$ \psi_*^{\lambda} ^2$	$\frac{1}{8\pi^2} J(\theta_1, \theta_2) $
$(0, 0)$	$(\frac{1}{6}, \frac{23}{24})$	$\frac{3-\sqrt{6}}{60}$	$\frac{3-\sqrt{6}}{\sqrt{3}}$
$(3, 0)$	$(\frac{7}{24}, \frac{5}{6})$	$\frac{3+\sqrt{6}}{60}$	$\frac{3+\sqrt{6}}{\sqrt{3}}$
$(0, 1)$	$(\frac{7}{24}, \frac{23}{24})$	$\frac{1}{4}$	$\sqrt{3}$
$(4, 0)$	$(\frac{1}{3}, \frac{19}{24})$	$\frac{1}{4}$	$\sqrt{3}$
$(1, 1)$	$(\frac{1}{3}, \frac{11}{12})$	$0, 0$	$2\sqrt{3}$

where the eigenvectors ψ^{λ} have been normalized so that $\|\psi^{\lambda}\| = 1$. In this case $60|\psi_*^{\lambda}|^2 = \sqrt{3}|J|/8\pi^2$ for $\lambda \in \{(0, 0), (3, 0)\}$ and $48|\psi_*^{\lambda}|^2 = 2J^2/64\pi^4$ for $\lambda \in \{(0, 1), (4, 0)\}$. Thus we have the following result:

Theorem 5.6. *The joint spectral measure of $\mathcal{E}_4^{M, \rho_1}(G_2)$, $\mathcal{E}_4^{M, \rho_2}(G_2)$ (over \mathbb{T}^2) is*

$$d\varepsilon = \frac{\sqrt{3}}{160\pi^2}|J| d^{(6,1/24)} + \frac{1}{2048\pi^4}J^2 d^{((6))} + \frac{1}{2048\pi^4}J^2 d^{((8/3))} - \frac{\sqrt{6}}{360} \sum_{g \in D_{12}} \delta_{g(e^{\pi i/4}, -i)}, \quad (54)$$

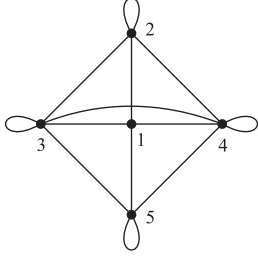


Figure 36: Graph $\mathcal{E}_4^{*,\rho_1}(G_2)$

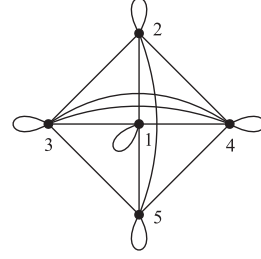


Figure 37: Graph $\mathcal{E}_4^{*,\rho_2}(G_2)$

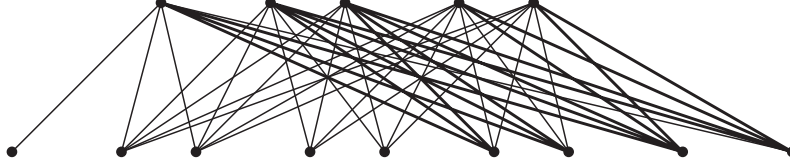


Figure 38: Expected principal graph of G_2 -GHJ subfactor with nimrep $\mathcal{E}_4^*(G_2)$

where $d^{((n))}$, $d^{(n,k)}$ are as in Definition 2.1 and δ_x is the Dirac measure at the point x .

5.6 Exceptional Graph $\mathcal{E}_4^*(G_2)$

The graphs $\mathcal{E}_4^{*,\rho_j}(G_2)$ are illustrated in Figures 36 and 37. To our knowledge the second graph $\mathcal{E}_4^{*,\rho_2}(G_2)$ has not appeared in the literature before in the context of nimrep graphs or subfactors. The associated modular invariant is [41, (5.1)]

$$\begin{aligned} Z_{\mathcal{E}_4^*} = & |\chi_{(0,0)}|^2 + |\chi_{(3,0)}|^2 + |\chi_{(1,1)}|^2 + |\chi_{(2,0)}|^2 + |\chi_{(2,1)}|^2 \\ & + \chi_{(1,0)}\chi_{(0,2)}^* + \chi_{(0,2)}\chi_{(1,0)}^* + \chi_{(0,1)}\chi_{(4,0)}^* + \chi_{(4,0)}\chi_{(0,1)}^* \end{aligned}$$

which is at level 4 and has exponents $\text{Exp}(\mathcal{E}_4^*(G_2)) = \{(0,0), (3,0), (1,1), (2,0), (2,1)\}$.

This modular invariant is a permutation invariant, and does not come from a conformal embedding. It has not yet been shown that the graphs $\mathcal{E}_4^{*,\rho_j}(G_2)$ arise from a braided subfactor. This will be discussed in a future publication using a generalised Goodman-de la Harpe-Jones construction (c.f. the comments in Section 5.3), which produces the second graph $\mathcal{E}_4^{*,\rho_2}(G_2)$ as a nimrep graph. It is expected that $\mathcal{E}_4^{*,\rho_j}(G_2)$ does indeed arise as the nimrep for a type II inclusion with index $39 + 16\sqrt{6} \approx 78.19$. The expected principal graph for this inclusion is illustrated in Figure 38, where the thick lines indicate double edges. Again, it is not clear what the dual principal graph is in this case.

However, for our purposes it is sufficient to know the eigenvalues and corresponding eigenvectors for these graphs, and it is not necessary for the graph to be a nimrep graph. For this graph there are two distinct vertices (up to an automorphism of the graph) which both have lowest Perron-Frobenius weight. These are numbered 1 and 2 in both Figures 36, 37. Here we compute the spectral measure where the distinguished vertex is one of these vertices, the vertex numbered 1. Choosing the other vertex with lowest Perron-Frobenius weight as the distinguished vertex would yield a different measure.

Then with θ_1, θ_2 as in (39) for $\lambda = (\lambda_1, \lambda_2) \in \text{Exp}(\mathcal{E}_4^*(G_2))$, we have:

$\lambda \in \text{Exp}$	$(\theta_1, \theta_2) \in [0, 1]^2$	$ \psi^\lambda ^2$
$(0, 0)$	$(\frac{1}{6}, \frac{23}{24})$	$\frac{1}{6}$
$(3, 0)$	$(\frac{7}{24}, \frac{5}{6})$	$\frac{1}{6}$
$(1, 1)$	$(\frac{1}{3}, \frac{11}{12})$	0
$(2, 0)$	$(\frac{1}{4}, \frac{7}{8})$	0
$(2, 1)$	$(\frac{3}{8}, \frac{7}{8})$	$\frac{2}{3}$

where again the eigenvectors ψ^λ have been normalized so that $\|\psi^\lambda\| = 1$. We have the following result:

Theorem 5.7. *A spectral measure of $\mathcal{E}_4^{*,\rho_1}(G_2)$, $\mathcal{E}_4^{*,\rho_2}(G_2)$ (over \mathbb{T}^2), with distinguished vertex $*$ = 1 in Figure 36, is*

$$d\varepsilon = \frac{1}{2}d^{(6,1/24)} + \frac{1}{18} \sum_{g \in D_{12}} \delta_{g(i, e^{3\pi i/4})}, \quad (55)$$

where $d^{(n,k)}$ is as in Definition 2.1 and δ_x is the Dirac measure at the point x .

Acknowledgement.

The second author was supported by the Coleg Cymraeg Cenedlaethol.

References

- [1] T. Banica and D. Bisch, Spectral measures of small index principal graphs, *Comm. Math. Phys.* **269** (2007), 259–281.
- [2] T. Banica and J. Bichon, Spectral measure blowup for basic Hadamard subfactors. arXiv:1402.1048 [math.OA].
- [3] J. Böckenhauer and D. E. Evans, Modular invariants, graphs and α -induction for nets of subfactors. II, *Comm. Math. Phys.* **200** (1999), 57–103.
- [4] J. Böckenhauer and D. E. Evans, Modular invariants, graphs and α -induction for nets of subfactors. III, *Comm. Math. Phys.* **205** (1999), 183–228.
- [5] J. Böckenhauer and D. E. Evans, Modular invariants from subfactors: Type I coupling matrices and intermediate subfactors, *Comm. Math. Phys.* **213** (2000), 267–289.
- [6] J. Böckenhauer and D. E. Evans, Modular invariants and subfactors, in *Mathematical physics in mathematics and physics (Siena, 2000)*, Fields Inst. Commun. **30**, 11–37, Amer. Math. Soc., Providence, RI, 2001.
- [7] J. Böckenhauer and D. E. Evans, Modular invariants from subfactors, in *Quantum symmetries in theoretical physics and mathematics (Bariloche, 2000)*, *Contemp. Math.* **294**, 95–131, Amer. Math. Soc., Providence, RI, 2002.
- [8] J. Böckenhauer, D. E. Evans and Y. Kawahigashi, On α -induction, chiral generators and modular invariants for subfactors, *Comm. Math. Phys.* **208** (1999), 429–487.
- [9] J. Böckenhauer, D. E. Evans and Y. Kawahigashi, Chiral structure of modular invariants for subfactors, *Comm. Math. Phys.* **210** (2000), 733–784.
- [10] P.F. Byrd and M.D. Friedman, *Handbook of elliptic integrals for engineers and scientists*, Die Grundlehren der mathematischen Wissenschaften, Band 67, Second edition, revised. Springer-Verlag, New York, 1971.
- [11] F. Calegari, S. Morrison and N. Snyder, Cyclotomic integers, fusion categories, and subfactors, *Comm. Math. Phys.* **303** (2011), 845–896.
- [12] P. Christe and F. Ravanani, $GN \otimes GN + L$ conformal field theories and their modular invariant partition functions, *Int. J. Mod. Phys. A* **4** (1989), 897–920.
- [13] R. Coquereaux, R. Rais and E.H. Tahri, Exceptional quantum subgroups for the rank two Lie algebras B_2 and G_2 , *J. Math. Phys.* **51** (2010), 092302 (34 pages)
- [14] P. Di Francesco, Integrable lattice models, graphs and modular invariant conformal field theories, *Internat. J. Modern Phys. A* **7** (1992), 407–500.
- [15] D. E. Evans, Fusion rules of modular invariants, *Rev. Math. Phys.* **14** (2002), 709–732.

- [16] D. E. Evans, Critical phenomena, modular invariants and operator algebras, in *Operator algebras and mathematical physics (Constanța, 2001)*, 89–113, Theta, Bucharest, 2003.
- [17] D. E. Evans and T. Gannon, Near-group fusion categories and their doubles, *Adv. Math.* **255** (2014), 586–640.
- [18] D. E. Evans and Y. Kawahigashi, *Quantum symmetries on operator algebras*, Oxford Mathematical Monographs. The Clarendon Press Oxford University Press, New York, 1998. Oxford Science Publications.
- [19] D. E. Evans and M. Pugh, Ocneanu Cells and Boltzmann Weights for the $SU(3)$ ADE Graphs, *Münster J. Math.* **2** (2009), 95–142.
- [20] D. E. Evans and M. Pugh, $SU(3)$ -Goodman-de la Harpe-Jones subfactors and the realisation of $SU(3)$ modular invariants, *Rev. Math. Phys.* **21** (2009), 877–928.
- [21] D. E. Evans and M. Pugh, Spectral Measures and Generating Series for Nimrep Graphs in Subfactor Theory, *Comm. Math. Phys.* **295** (2010), 363–413.
- [22] D. E. Evans and M. Pugh, Spectral Measures and Generating Series for Nimrep Graphs in Subfactor Theory II: $SU(3)$, *Comm. Math. Phys.* **301** (2011), 771–809.
- [23] D. E. Evans and M. Pugh, Spectral Measures for G_2 II: finite subgroups. Preprint, arXiv:1404.1866 [math.OA].
- [24] D.E. Evans and M. Pugh, Spectral Measures for C_2 and B_2 . Preprint, arXiv:1404.1912 [math.OA].
- [25] D.E. Evans and M. Pugh, Spectral measures associated to rank two Lie groups and finite subgroups of $GL(2, \mathbb{Z})$. Preprint, arXiv:1404.1877 [math.OA].
- [26] T. Gannon, Algorithms for affine Kac-Moody algebras. arXiv:hep-th/0106123.
- [27] T. Gannon and Q. Ho-Kim, The low level modular-invariant partition functions of rank-two algebras, *Internat. J. Modern Phys. A* **9** (1994), 2667–2686.
- [28] R. Gaskell, A. Peccia and R.T. Sharp, Generating functions for polynomial irreducible tensors, *J. Mathematical Phys.* **19** (1978), 727–733.
- [29] M. Izumi, The structure of sectors associated with Longo-Rehren inclusions. II. Examples, *Rev. Math. Phys.* **13** (2001), 603–674.
- [30] V. F. R. Jones, The annular structure of subfactors, in *Essays on geometry and related topics, Vol. 1, 2*, Monogr. Enseign. Math. **38**, 401–463, Enseignement Math., Geneva, 2001.
- [31] V.F.R. Jones, S. Morrison and N. Snyder, The classification of subfactors of index at most 5, *Bull. Amer. Math. Soc. (N.S.)* **51** (2014), 277–327.
- [32] V.G. Kač and D.H. Peterson, Infinite-dimensional Lie algebras, theta functions and modular forms, *Adv. in Math.* **53** (1984), 125–264.
- [33] M. Nesterenko, J. Patera and A. Tereszkievich, Orthogonal polynomials of compact simple Lie groups, *Int. J. Math. Math. Sci.* **2011**, Art. ID 969424, 23 pp.
- [34] A. Ocneanu, Paths on Coxeter diagrams: from Platonic solids and singularities to minimal models and subfactors. (Notes recorded by S. Goto), in *Lectures on operator theory*, (ed. B. V. Rajarama Bhat et al.), The Fields Institute Monographs, 243–323, Amer. Math. Soc., Providence, R.I., 2000.
- [35] A. Ocneanu, Higher Coxeter Systems (2000). Talk given at MSRI. <http://www.msri.org/publications/ln/msri/2000/subfactors/ocneanu>.
- [36] A. Ocneanu, The classification of subgroups of quantum $SU(N)$, in *Quantum symmetries in theoretical physics and mathematics (Bariloche, 2000)*, *Contemp. Math.* **294**, 133–159, Amer. Math. Soc., Providence, RI, 2002.
- [37] K.-H. Rehren, Space-time fields and exchange fields, *Comm. Math. Phys.* **132** (1990), 461–483.
- [38] P. Ruelle, Invariance modulaire dans les theories de champs conformes bidimensionnelles, PhD thesis, Louvain-la-Neuve, 1990.
- [39] M. Takesaki, *Theory of operator algebras. I*, *Encyclopaedia of Mathematical Sciences* **124**. Springer-Verlag, Berlin, 2002.
- [40] S. Uhlmann, R. Meinel and A. Wipf, Ward identities for invariant group integrals, *J. Phys. A* **40** (2007), 4367–4389.
- [41] D. Verstegen, New exceptional modular invariant partition functions for simple Kac-Moody algebras, *Nuclear Phys. B* **346** (1990), 349–386.
- [42] D. V. Voiculescu, K. J. Dykema and A. Nica, *Free random variables*, CRM Monograph Series **1**, American Mathematical Society, Providence, RI, 1992.
- [43] H. Weyl, Theorie der Darstellung kontinuierlicher halb-einfacher Gruppen durch lineare Transformationen, *Math. Z.* **23** (1925), 271–309, **24** (1926), 328–395.
- [44] F. Xu, New braided endomorphisms from conformal inclusions, *Comm. Math. Phys.* **192** (1998), 349–403.
- [45] F. Xu, Unpublished notes, 2001.